

# **VAPOUR PHASE STUDY OF *m*-XYLENE ISOMERIZATION USING NICKEL HYDROGEN MORDENITE CATALYST**

A thesis submitted  
in Partial Fulfilment of the Requirements  
for the degree of

**MASTER OF TECHNOLOGY**

by

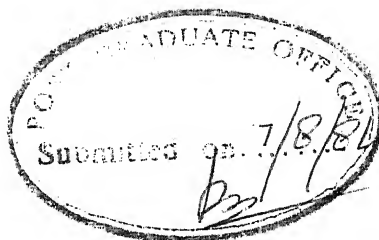
**V. SREEDHARAN**

to the

**DEPARTMENT OF CHEMICAL ENGINEERING  
INDIAN INSTITUTE OF TECHNOLOGY, KANPUR**


**AUGUST 1984**

CERTIFICATE.



This is to certify that the present work, "VAPOUR  
PHASE STUDY OF m-XYLENE ISOMERIZATION USING NICKEL HYDROGEN  
MORDENITE CATALYST" has been carried out under my supervision  
and that this has not been submitted elsewhere for a degree.

August 7, 1984

  
Dr. S. Bhatia 7/8/84.  
Assistant Professor  
Department of Chemical Engineering  
Kanpur-208016 India

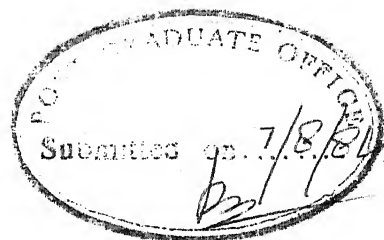
POST GRADUATE OFFICE  
This thesis has been approved  
for the award of the Degree of  
Master of Technology (M.Tech.)  
in accordance with the  
regulations of the Indian  
Institute of Technology Kanpur  
Dated. 12/8/84. 2

CHE-1984-M-SRE-VAP

83957

21 SEP 1984

CERTIFICATE.



This is to certify that the present work, "VAPOUR PHASE STUDY OF m-XYLENE ISOMERIZATION USING NICKEL HYDROGEN MORDENITE CATALYST" has been carried out under my supervision and that this has not been submitted elsewhere for a degree.

August 7, 1984

  
7/8/84.

Dr. S. Bhatia  
Assistant Professor  
Department of Chemical Engineering  
Kanpur-208016 India

**POST GRADUATE OFFICE**

This thesis has been approved  
for the award of the Degree of  
Master of Technology (M.Tech.)  
in accordance with the  
regulations of the Indian  
Institute of Technology Kanpur  
Dated. 13/8/84. 2

## ACKNOWLEDGEMENTS

I would like to take this opportunity to express my deep sense of gratitude to Dr. S. Bhatia for his inspiring guidance, valuable advice and meticulous attention throughout the development of this work. It was really a pleasant experience to have worked with him.

I am very much thankful to a host of my friends for their timely help and co-operation during the course of this work.

Thanks are also due to Mr. J.S. Virdi for helping me with the fabrication of the experimental setup. I am also thankful to Mr. Sanjeev Rao, Mr. N.P. Singh & Mr. Ramchandra Ram for their help during the course of this work.

Thanks to Mr. Raj Khanna for his neat typing, Mr. J.C. Verma for his neat tracing of figures, Mr. D.B. Chakravorty for xeroxing & Mr. Hari Ram for cyclostyling the thesis.

V. SREEDHARAN

# CONTENTS

	Page
List of Figures	vi
List of Tables	viii
Nomenclature	ix
Abstract	xi
 CHAPTER	
1 Introduction	1
2 Literature survey	4
3 Experimental	16
3.1 Catalyst supports and chemicals	16
3.2 Catalyst preparation	16
3.3 Experimental setup	17
3.4 Experimental procedure	19
3.5 Product analysis	20
3.6 X-ray diffraction studies	22
4 Results and Discussion	24
4.1 Mass transfer effects	25
4.1.1 Effect of space velocity	26
4.1.2 Effect of catalyst particle size	26
4.2 Activity and selectivity studies	31
4.2.1 Effect of $H_2$ /m-xylene mole ratio	32
4.2.2 Effect of LHSV	32
4.2.3 Effect of reaction temperature	35
4.2.4 Effect of nickel content	39
4.2.5 Effect of nickel crystallite size	44
4.3 Reaction kinetics and modelling	49
4.3.1 Mathematical modelling & data analysis	58
5 Conclusions and Recommendations	65

5.1	Conclusions	65
5.2	Recommendations	66
	References	68
	Appendix A	71
	Appendix B	72

# LIST OF FIGURES

Figure		Page
1	Mordenite framework structure	9
2	General composition of zeolon materials	9
3	Experimental setup	18
4	Typical chromatogram showing product distribution for m-xylene isomerization over 1.5% Ni-HW catalyst at 598 K	21
5	Effect of space velocity on m-xylene conversion	27
6	Effect of catalyst particle size on m-xylene conversion	28
7	Effect of H <sub>2</sub> /m-xylene mole ratio on conversion, isomerization activity and selectivity	33
8	Effect of LWHSV on isomerization activity and conversion of meta to para and ortho isomers	34
9	Effect of reaction temperature on conversion, isomerization activity and selectivity	36
10	Effect of reaction temperature on conversion of meta to para and ortho isomers	38
11	Effect of nickel content on conversion isomerization activity and selectivity	41
12	Effect of nickel crystallite size on m-xylene conversion and turnover number	46
13	Effect of nickel metal area on turnover number	47
14	Effect of partial pressure of m-xylene on conversion at different reaction temperatures	56

15	Effect of partial pressure of m-xylene on p-xylene selectivity at different reaction temperatures	57
16	Plot of experimental rate vs theoretical rate for the reaction of meta to para isomer at different temperatures	60
17	Plot of experimental rate vs theoretical rate for the reaction of meta to ortho at different temperatures	61
18	Effect of reaction temperature on reaction rate constants (Arrhenius plot)	63

LIST OF TABLES

Table		Page
1	Comparison of reaction rates of different catalyst particle sizes	30
2	Comparison of activity and p-xylene selectivity of various catalysts	40
3	Nickel crystallite size, metal surface area and turnover number of Ni-HM catalysts	43
4	Summary of rate models tested	54
5	Rate constants and adsorption equilibrium constants of m-xylene isomerization on 1.5% Ni-HM catalyst at different temperatures	62
6	Comparison of activation energies with reported values for the isomerization reaction	64

## NOMENCLATURE

$d_v$	=	Volume average crystallite diameter, nm
$K_o$	=	Crystallite shape factor, dimensionless
$K, K'$	=	Homogeneous reaction equilibrium constants for the reactions, meta to ortho & meta to para isomers respectively, dimensionless
A	=	meta xylene
R	=	ortho xylene
S	=	para xylene
$k_A, k_R, k_S$	=	Rate constants for adsorption of A, R or S on catalyst surface, g.mol/(hr)(g.catalyst )
$k, k'$	=	overall rate constants for the reactions, meta to ortho & meta to para respectively, g.mol/(hr)(g.catalyst)
$K_A, K_R, K_S$	=	Adsorption equilibrium constants for components A, R, S respectively, (atm <sup>-1</sup> )
$r_R$	=	Rate of isomerization of m-xylene to p-xylene, g.mol/(hr.(g.catalyst))
$r_S$	=	Rate of isomerization of m-xylene to p-xylene, g.mol/(hr)(g.catalyst)
$r_1$	=	Rate of reaction of any particle size, g.mol/(hr)(g.catalyst)
$r_2$	=	Rate of reaction of powdered catalyst, g.mol/(hr)(g.catalyst)
LWHSV	=	Liquid weight hourly space velocity, hr <sup>-1</sup>
F	=	m-xylene feed rate, g.mol/hr
W	=	Weight of catalyst, g
s	=	Specific metal surface area

$X_R$  = Conversion of m-xylene to o-xylene

$X_S$  = Conversion of m-xylene to p-xylene

Greek Symbols :

$\mu_{1/2}$  = Width of nickel peak at half maximum intensity, radians

$\lambda$  = Wavelength of X-ray radiation, nm

$\eta$  = Effectiveness factor, dimensionless

$\theta$  = Bragg's angle, radians

ABSTRACT

Kinetics of m-xylene isomerization has been studied in vapour phase over nickel hydrogen mordenite (Ni-HM) catalyst. Catalyst was prepared by impregnation technique and the reaction was carried out in hydrogen atmosphere in a fixed bed flow reactor. Nickel content of the catalyst was varied from 0.5% to 5% by weight. Mass transfer effects were found to be negligible. Activity and selectivity of the catalyst were affected by  $H_2$ /m-xylene mole ratio, liquid weight hourly space velocity (LWHSV), reaction temperature, nickel content and nickel crystallite size. 1.5% nickel hydrogen mordenite gave maximum conversion and activity.

A ~~separallèle~~ reaction scheme with no interconversion between ortho & para isomers was proposed for the reaction. The kinetic data were analysed on the basis of Langmuir-Hinshelwood kinetics with statistical data interpretation. The rate controlling step in the over all kinetics of the reaction was dual site surface reaction model. The activation energy values were 17.61 kcal/mol for p-xylene formation and 15.28 kcal/mol for o-xylene formation respectively.

## CHAPTER 1

### INTRODUCTION

At the start of the 20th century the only use of xylene was as a component of solvent naphtha. At around 1920 the xylenes found their utilization in the dye industry as a component for lacquers. During this period the antiknock properties of xylenes were discovered. The usage of individual isomers ortho, meta and para xylenes were not recognized until the middle of 20th century when methods of separation of the individual isomers were developed. In 1955 the commercial utilization of the isomer para xylene started as the raw material for production of polyester fibres and films. In 1960, the use of ortho xylene began in the manufacture of alkyd resins, an important component in making hard durable lacquers. The main component of these resins, phthalic anhydride could be obtained by oxidation of naphthalene or ortho xylene. Now, with the great reduction in the quantity of naphthalene available, the demand of ortho xylene for this purpose has increased many fold. Another important use of phthalic anhydride is as an intermediate in the manufacture of plasticizers.

The above mentioned uses along with many others placed the para and ortho xylenes as a basic raw material in a key position of importance in the petrochemical industry.

It is a paradox that m-xylene has got the least demand inspite of it being present in the largest amount as a product from the catalytic reforming of petroleum naphtha. Meta xylene can be oxidized to isophthalic acid which is used for the production of unsaturated polyesters but the tonnage employed is very small. The bulk of the meta xylene has to be used as a blend in motor gasoline. So, as far as economics and demand of the isomers are concerned, if m-xylene can be isomerized successfully to o- and p-xylenes, it will be of great advantage.

The isomerization of xylenes is generally carried out in the presence of an acid catalyst (1-3). The reaction can be affected in both liquid and vapour phase. The liquid phase isomerization using homogeneous acid-halide catalysts suffer from corrosion and recovery problems. The vapour phase isomerization on heterogeneous silica alumina and dual function type catalysts avoids these problems of homogeneous catalysts but the high temperature required leads to coke formation, thereby affecting the yield of the desired product by poisoning the catalyst. Addition of hydrogen to the xylene feed reduces coke formation, suppresses side reactions and increases the rate of xylene isomerization.

In recent years, the aromatic isomerization reactions are studied using various zeolite catalysts because of their better activity and selectivity compared to silica alumina and

homogeneous acid halide catalysts. Metals were dispersed on these supports to obtain better yield and selectivity of products. Platinum has been extensively used for this purpose.

Hydrogen mordenite has been reported as a catalyst for xylene isomerization in liquid phase (4,5) and vapour phase (6). Nickel supported catalysts were used for isomerization of paraffins (7). In view of these facts it is possible that nickel supported over mordenite may show considerable catalytic activity for the isomerization of m-xylene.

The aim of the present study was to obtain xylene isomerization rate data using nickel hydrogen mordenite (Ni-HM) as the catalyst and to compare these data with reported values in the literature for different catalysts. The isomerization reaction was carried out in the vapour phase using nickel supported mordenite catalyst. Nickel was supported on hydrogen mordenite by impregnation technique and reduced to nickel metal in the presence of flowing hydrogen gas. The reaction was carried out in a fixed bed reactor under hydrogen atmosphere to keep the catalyst free from coke formation throughout the reaction. Effect of liquid weight hourly space velocity (LWHSV), reaction temperature, nickel concentration and nickel crystallite size were the important variables studied for isomerization activity and selectivity of the catalyst. The kinetic data were analyzed using a model based on Langmuir Hinshelwood kinetics.

## CHAPTER 2

### LITERATURE SURVEY

Xylene isomerization has been studied by a number of research workers in the past. Various types of catalysts were employed for the reaction. These are briefly discussed below.

The isomerization of xylene is greatly aided by the use of an acid catalyst and can be carried out in either the liquid phase or vapour phase. Thermal isomerization of xylenes is of very little interest because extreme conditions are required and the yields are very poor (8). The liquid phase isomerization of xylenes can be carried out under either homogeneous or heterogeneous conditions with a combination of Lewis acids as a catalyst, for example,  $\text{HF}/\text{BF}_3$ . Such reactions have been observed to be first order with respect to xylene concentration (2,3) and first order with respect to catalyst concentration for homogeneous phase conditions (2).

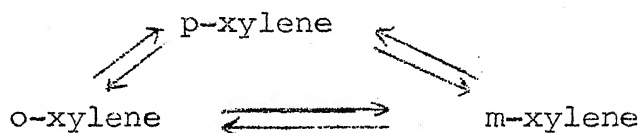
Most of the earlier studies of liquid phase isomerization of xylene were carried out using homogeneous acid halide catalyst. McCaulay and Lien (1) studied the isomerization reaction using hydrogen bromide and boron trifluoride as catalysts and found that the extent of isomerization reaction strongly depended upon the boron trifluoride concentration. Brown and Jungk (2) reported the values for rate constants and activation energies for the

isomerization reaction using hydrogen bromide and aluminium bromide as catalyst. They also proposed that the reaction would be occurring via series mechanism i.e., p-xylene  $\rightleftharpoons$  m-xylene  $\rightleftharpoons$  o-xylene. The reaction followed second order kinetics, first order with respect to both xylene and catalyst concentration. Similar results were reported by Allen and Yats (3). The disproportionation of xylenes to toluenes and trimethyl benzenes, a major side reaction was suppressed using toluene as a diluent. The usage of homogeneous acid-halide catalysts in the liquid phase isomerization suffers from various drawbacks such as side reactions, sludge formation, loss of partially soluble catalyst, corrosion and difficulty in recovery of products.

Due to the above problems of liquid phase catalyst-reaction system interest has turned towards acidic type heterogeneous catalysts such as silica alumina. Unfortunately, these catalysts are not very active at the ordinary temperature and therefore high temperatures are needed for these catalysts to achieve considerable amount of catalytic activity. Most of the studies were carried out in vapour phase. The vapour phase isomerization of xylene over silica alumina catalysts were studied by number of workers (9-17).

Hanson and Engel (16) reported the kinetics of vapour phase isomerization over silica alumina catalyst. They found that m-xylene isomerizes reversibly to o-xylene and p-xylene

over silica alumina, but direct interconversion between o-xylene and p-xylene does not occur. Xylene isomerization was found to be first order and was described by a single site rate model. The values of rate constants and activation energies were reported for isomerization as well as disproportionation. The activity of silica alumina catalyst for isomerization of xylenes was found to be strongly dependent on the combined effect of time, temperature and gaseous environment. Cortes and Corma (17) investigated the mechanism and kinetics of vapour phase isomerization of xylenes over silica alumina catalyst. Silvestri and Prater (15) investigated the kinetics of the selectivity of gas phase xylene isomerization over silica alumina catalyst. They proposed a coupled reaction scheme involving six rate constants



where they considered the interconversion among the three isomers. The coupled reaction network is difficult to solve since it is seldom possible to obtain absolute rates for the three reactants due to catalyst aging, unknown catalyst site density etc. Fortunately, a method developed by Wei and Prater (18) permits reduction of the coupled reaction network to an uncoupled network. This mathematical method permits one to

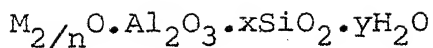
calculate the six rate constants without the need to obtain absolute conversion rates for any of the three reactions.

Silica alumina alone is not very efficient for the isomerization reaction. To enhance the activity and selectivity of the reaction, various metals supported on silica-alumina are used as catalysts. Platinum is extensively used for this purpose. Isomerization activity of the xylenes over a platinum containing silica alumina catalyst was improved by coupling with a recycle of product system (13). Isomerization of o- and p-xylenes over a bifunctional  $\text{Pt/SiO}_2\text{-Al}_2\text{O}_3$  catalyst studied in a temperature range of 703K to 748K indicated that m-xylene was an intermediate in both the forward and backward reaction (11). A catalyst containing platinum, rhodium and tin over  $\gamma$ -alumina showed more than 80% conversion of m-xylene to p-xylene (14).

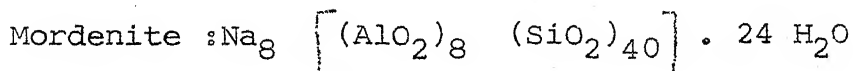
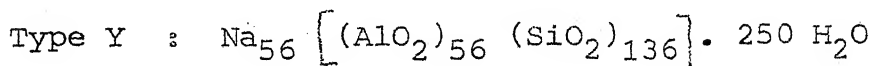
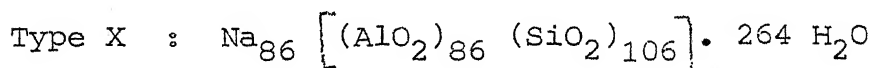
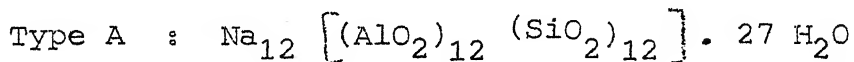
Activities of various zeolite catalysts were established long back for the paraffin isomerization reaction. These catalysts have shown higher activity and selectivity for the aromatic isomerization reaction. Infact, in recent years, most of the xylene isomerization studies have been carried out on various zeolite catalysts which showed considerable improvements over the silica alumina and the homogeneous acidic halide catalysts as far as activity and selectivity are concerned.

Synthetic zeolites or molecular sieves have a general

formula as :



where, M is a cation of valence n. The framework structure contains channels and interconnected voids which are occupied by the cation and water molecules. The cations are quite mobile and may be exchanged to varying degrees by other cations. The intercrystalline water can be removed reversibly for some zeolites. The mordenite framework structure is shown in Fig. 1. There are various types of zeolites but the most commercially useful zeolites are A type, X type, Y type and mordenite. The unit cell representation of these zeolites are (35) :



The molecular sieves can be located on the three phase (silica-alumina-alkali) compositional diagram as shown in figure 2. In general, the acid resistance increases as the silica content increases. Molecular sieves based on mordenite material with a silica-alumina ratio of 10:1 have much more chemical and thermal stabilities than those having lower silica-

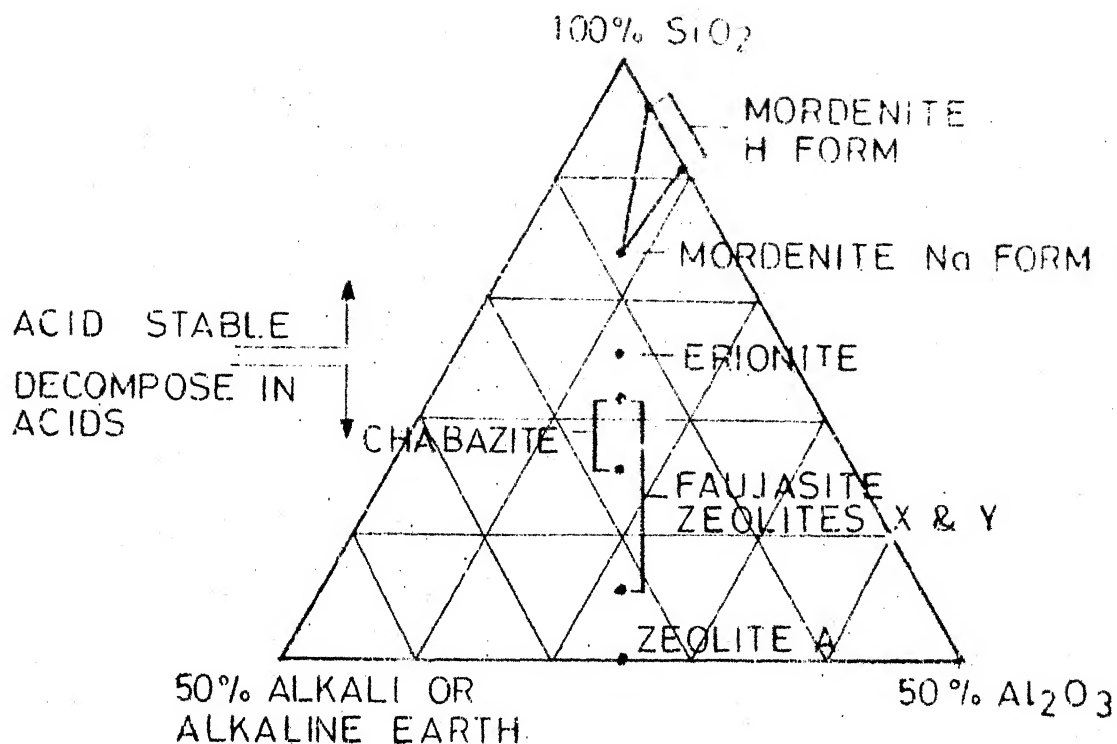


FIG.2 GENERAL CHEMICAL COMPOSITION OF ZEOLON MATERIALS

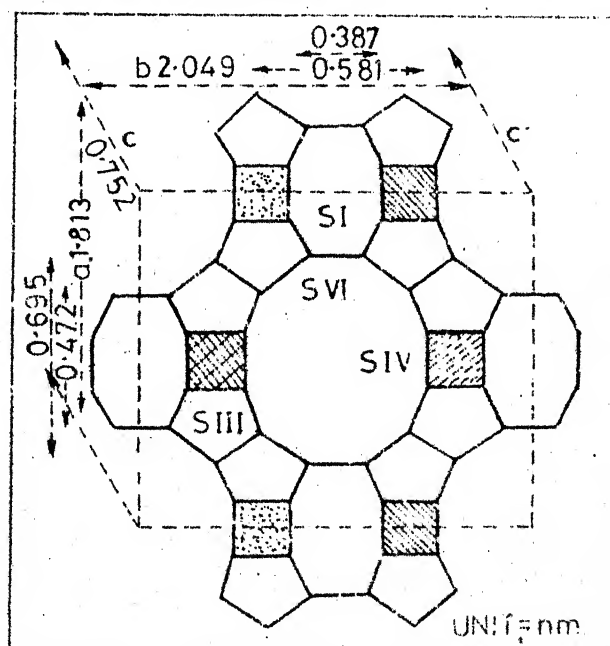


FIG.1 MORDENITE FRAMEWORK STRUCTURE

CO-PLANAR FACES

UNIT

alumina ratio.

A number of studies are reported in the literature for isomerization of xylenes over zeolite catalysts. Hansford and Ward (19) found higher isomerization activity of zeolite catalysts compared to silica-alumina catalysts. Catalyst acidity played an important role in the activity of the catalyst. Spectroscopic studies indicated that the catalytic activity of aluminosilicates for m-xylene isomerization depends on the concentration of strongly acidic centres (20). Bremar et al. (21) revealed that the catalytically active centres in xylene isomerization are Bronsted acid centres which occur on cation exchanged zeolites by dissociation adsorption of  $H_2O$  molecules if the polarizing effect of the cations is sufficiently strong and the cations are not saturated sterically or bonded by the zeolite skeleton. Experiments conducted by Sharma et al. (22) on o-xylene isomerization with various forms of X-zeolites showed that calcium-X and hydrogen-X possessing stronger acid sites were more active than sodium-X which contains only weak acid sites.

To obtain greater activity, the acidity of the zeolites can be increased by increasing the silica/alumina ratio. This can be achieved by dealuminating the zeolite. Gajewski et al. (23) obtained higher activity of the Al-deficient zeolite (dealumina Y-zeolite) in m-xylene isomerization. Parasiewicz et al. (24)

used series of X and Y zeolites in the Lanthanum (La), calcium (Ca), magnesium (Mg) and hydrogen (H) forms as catalyst for m-xylene isomerization. Best activity was exhibited by dealuminated mordenite containing 20:1 silica-alumina ratio in the hydrogen form which gave around 40% para and ortho xylenes with 80% selectivity at 473°K. The pore structure of mordenite was found to be an important factor for the process studied. Papp and Miklosy (25) found that the catalytically active centres of hydrogen mordenite for xylene isomerization reaction were the OH groups. 1,2 methyl group shift was found to be the mechanism of reaction. Hopper and Shigemura (4) obtained good isomerization activity and selectivity for o-xylene isomerization in liquid phase over hydrogen mordenite catalyst using toluene as diluent. First order kinetics was applied to fit the model satisfactorily. Norman et al. (5) investigated the kinetics of liquid phase isomerization of xylene over hydrogen mordenite. A Langmuir-Hinshelwood kinetic model was developed for the isomerization of xylene which assumes first order interconversion among the three isomers. This model is very comprehensive as it includes the effects of feed composition, catalyst activity, and temperature. The effect of composition was included in the reaction rate equation by the Langmuir-Hinshelwood expression which contains separate adsorption parameters and reaction rate parameters. The value of activation energy was reported.

Lanewala & Bolton (26) proposed that xylene isomerization occurred by the transalkylation mechanism. The isomerization of xylenes over a zeolite catalyst is invariably accompanied by transalkylation and the degree of isomerization is proportional to the extent of transalkylation. They proposed that the reaction proceeds via a bimolecular mechanism involving diphenyl type transition state. Using the monomolecular rate theory developed by Wei and Prater, Chutoransky & Dwyer (27) analyzed the kinetics of the liquid phase isomerization of xylene over a zeolitic catalyst. The kinetic analysis was presented primarily in terms of the time independent selectivity kinetics. It was found that the isomerization is a simple series reaction  $\text{o-xylene} \rightleftharpoons \text{m-xylene} \rightleftharpoons \text{p-xylene}$ . Collins et al. (28) investigated xylene isomerization and disproportionation over Lanthanum Y catalyst. A coupled reaction scheme involving six rate constants was proposed. The relative rates of the isomerization reactions were calculated using Wei-Prater method. The results were found to be consistent with a series reaction path for the isomerization reaction. Collins and Medina (29) studied xylene isomerization using ZSM-5 zeolite catalyst. They found that disproportionation was not a significant reaction in the temperature range of 523-623K. The relative rate constants calculated using Wei-Prater technique appeared to be influenced by diffusion and/or shape selectivity. ZSM-5 catalyst showed

a slight selectivity for p-xylene formation during xylene isomerization. This was believed to be due to shape selective diffusion.

Miklosy et al. (6) studied xylene isomerization on H-forms of natural mordenite and clinoptilolite, prepared by one of the following procedures : (i) acid treatment (ii)  $\text{NH}_4^+$  exchange followed by deammoniation and (iii)  $\text{Ag}^+$  exchange followed by reduction with hydrogen. They reported that the active sites for xylene isomerization are the acidic OH groups on the outer crystal surface of the H-forms of mordenites and clinoptilolite prepared differently. Bronsted centres of different activity, selectivity and stability are formed upon treatment with hydrochloric acid, or ammonium ion-exchange followed by thermal deammoniation, or silver ion exchange followed by reduction with hydrogen. H-forms of different zeolites prepared similarly showed different catalytic behaviour, thus indicating the effect of the lattice structure. The highest activity without deactivation was attained with the H(Ag)-form of natural small port mordenite, which contains accessible Bronsted acid sites in maximum concentration with maximum efficiency and stability. Thus the kinetics of isomerization could be investigated reliably on this catalyst.

On this catalyst the isomerization is a consecutive monomolecular transformation corresponding to the scheme  
 o-xylene  $\rightleftharpoons$  m-xylene  $\rightleftharpoons$  p-xylene. The kinetic order

varies between zero and unity, indicating a medium coverage of active sites. In terms of the Langmuir-Hinshelwood kinetics, the rate determining steps are the surface reactions, in which the shift of methyl groups to neighbouring positions take place in the adsorbed species, which is presumably a benzenium ion. The reactivities of xylene isomers do not differ substantially. The adsorption equilibrium constants of the isomers are in the same order of magnitude and their values affect the conversion rates only to a small extent.

Recently much of research works on xylene isomerization is directed towards getting high para selectivity for this reaction. Mostly investigated catalysts in this field are the ZSM-5 type. These catalyst supports have pore dimensions greater than the critical dimension of p-xylene but very close to those of m- and o-xylenes thereby lowering the m- and o-xylene diffusivities to a value much lower than that of p-xylene and thus giving rise to high para selectivity. A ZSM-5 catalyst (29) was found to yield a para/ortho ratio of 1.6 in the isomerization of m-xylene. A significant extent of disproportionation was also observed. A HZSM-5 catalyst containing platinum & Tin (30) gave para selective isomerization of mixed xylenes. But at the same time some amount of  $C_2-C_5$  hydrocarbons, benzene and toluene were formed as side products. The tin present in the catalyst was believed to suppress hydrogenation of the benzene ring.

Use of nickel metal loaded zeolites for the isomerization of n-paraffins have been studied for a long time. Burch (7) studied the isomerization of n-hexane on  $\text{Ni}/\text{Al}_2\text{O}_3$  catalyst. Minachev et al. (31) reported good activity for isomerization of butanes over nickel-hydrogen mordenite catalyst. Beecher & Voorhies (32) reported paraffin isomerization over a hydrogen mordenite based catalyst and concluded that the mordenite based catalysts are more active than faujasite based catalysts for these reactions. Similar observations were made by Inou & Sato (33) for xylene isomerization reaction. They found better activity and selectivity of mordenite based catalysts than amorphous silica-alumina & Y-type zeolites for isomerization of xylene.

Sensarma (34) studied the isomerization of m-xylene in the liquid phase over nickel hydrogen mordenite. 1.5% nickel hydrogen mordenite gave the maximum conversion and activity.

It appears from the literature that nickel hydrogen mordenite catalyst has not been studied extensively for vapour phase m-xylene isomerization. It is believed that this catalyst will show better catalytic activity and higher isomerization selectivity. Moreover, limited information is available regarding the kinetic study of this reaction using mordenite as a support. A detailed study of m-xylene isomerization including its kinetics has been undertaken using nickel supported mordenite catalyst.

## CHAPTER 3

### EXPERIMENTAL

#### 3.1 Catalyst supports and chemicals

Zeolite hydrogen mordenite (Zeolon 900 H) was obtained from M/s. Norton Chemicals, England. Typical physical characteristics of this zeolite are :

SiO <sub>2</sub> /Al <sub>2</sub> O <sub>3</sub>	:	10
Cation	:	H
Effective pore diameter:		8-9 Å
Bulk packing density	:	0.64-0.72 g/cc
Surface area	:	400 - 450 m <sup>2</sup> /g

Pure grade m-xylene was obtained from M/s. Reidel-De HaENAG Seelze Hannover . The purity of m-xylene was checked by GLC and was more than 99.5%. Anal R grade nickel nitrate was obtained from M/s. Thomas Baker & Co., Bombay. Technical grade hydrogen and nitrogen (99.5%) gases were supplied by M/s. Indian Oxygen Limited, Kanpur.

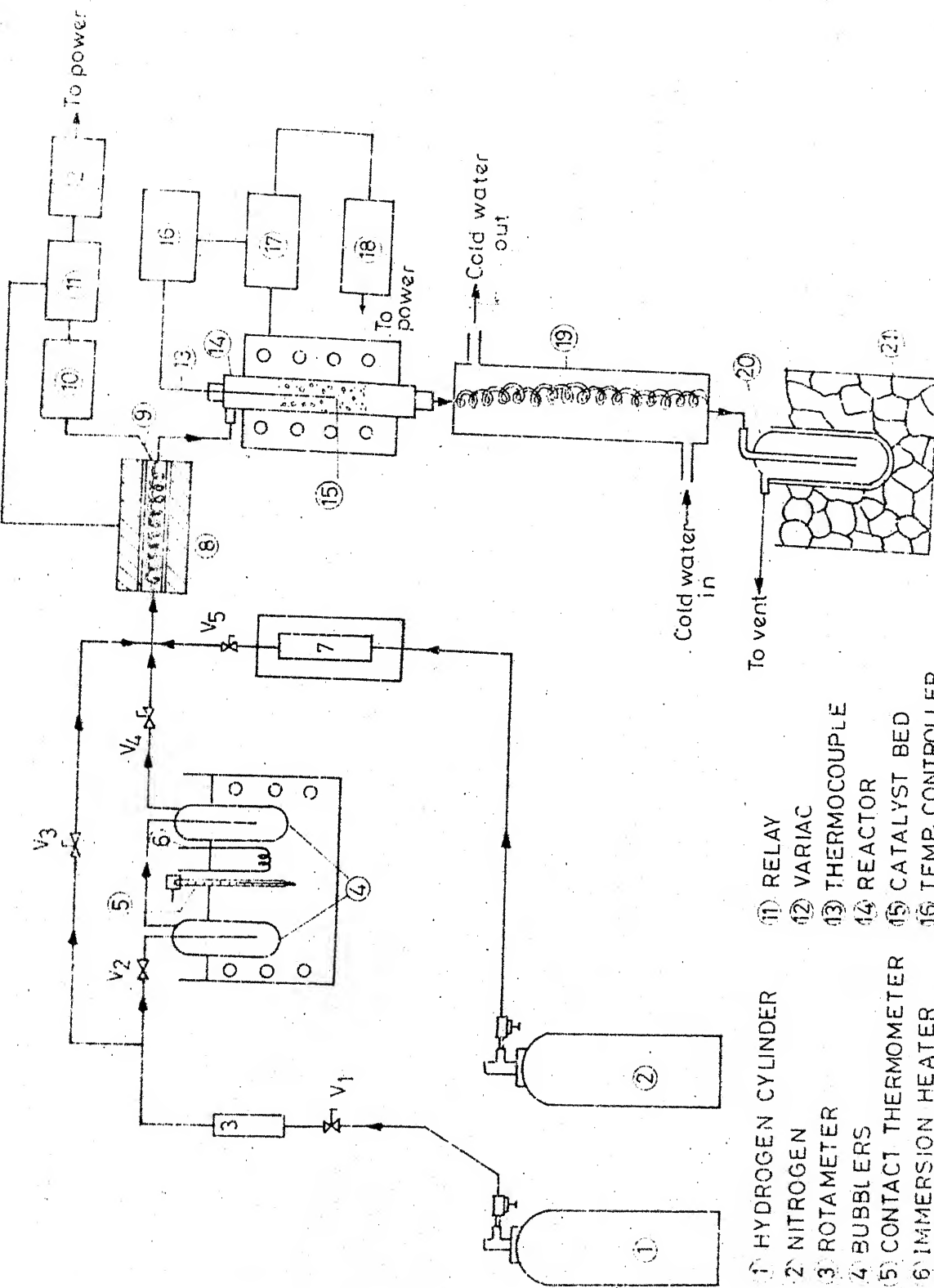
#### 3.2 Catalyst preparation

The nickel-hydrogen mordenite (Ni-HM) catalysts containing nickel metal on hydrogen mordenite was prepared by impregnation technique (36) as described below.

The amount of water absorbed by the support material (grams water absorbed per gram support) was first determined. Standard nickel nitrate solution was prepared using double distilled water. The amount of standard nickel nitrate solution to be impregnated was calculated for the preparation of a catalyst of known nickel percentage. This total amount of solution was impregnated in several instalments. In each instalment, appropriate amount of solution, equal to the amount that can be absorbed by the support was added in a rotary evaporator. The rotary evaporator was maintained at a constant temperature of  $383 \pm 1\text{K}$ . After the requisite amount of solution was added the material was dried in an oven maintained at  $393 \pm 5\text{K}$ . The catalysts were subsequently calcined at  $823\text{ K}$  in a muffle furnace for 20 hrs. The catalysts were reduced in situ in flowing hydrogen (40 ml/min) at a temperature of  $673\text{ K}$  for 15 hrs. The reduced catalysts were cooled to room temperature in hydrogen atmosphere.

### 3.3 Experimental setup

Isomerization of m-xylene was carried out in a fixed bed flow reactor. A schematic diagram of the setup is shown in Figure 3. The hydrogen/m-xylene mixture, used as reactants, was obtained by bubbling hydrogen through two bubblers arranged in series containing m-xylene kept in a constant temperature bath at a temperature of  $364 \pm 1\text{K}$  to have a



- ① HYDROGEN CYLINDER
- ② NITROGEN
- ③ ROTAMETER
- ④ BUBBLERS
- ⑤ CONTACT THERMOMETER
- ⑥ IMMERSION HEATER
- ⑦ ROTAMETER
- ⑧ PREHEATER
- ⑨ THERMOCOUPLE
- ⑩ TEMP. CONTROLLER

- ⑪ RELAY
- ⑫ VARIAC
- ⑬ THERMOCOUPLE
- ⑭ REACTOR
- ⑮ CATALYST BED
- ⑯ TEMP. CONTROLLER
- ⑰ RELAY
- ⑱ VARIAC
- ⑲ CONDENSER
- ⑳ LIQUID SAMPLER

⑳ ICE BATH  
 $V_1, V_2, V_3, V_4, V_5$ : VALVES

FIG.3 EXPERIMENTAL SETUP

desired hydrogen/m-xylene ratio. The reaction mixture was preheated in a tubular furnace which was controlled within an accuracy of  $\pm 5K$  by an IBP temperature controller using iron constantan thermocouple. The reaction mixture was passed through the reactor. The reactor was heated in a tubular furnace. The temperature of the catalyst bed was controlled within an accuracy of  $\pm 1K$  by an APLAB temperature controller using chromel-Alumel thermocouple placed centrally in the reactor.

### 3.4 Experimental procedure

#### 3.4.1 Activity and selectivity study :

3.0 g of a catalyst sample was charged in the reactor. The catalyst was reduced in situ in the reactor in flowing hydrogen (40 ml/min) for 15 hrs. before any activity measurements were made. The reaction temperature was adjusted to the desired value. The hydrogen flow rate was set at 32 ml/min and allowed to stabilize for half an hour. The hydrogen/m-xylene mixture was allowed to pass through the catalyst bed. Liquid samples were collected after 2 hrs once the steady state was attained.

#### 3.4.2 Kinetic study :

Kinetic study was performed under differential conditions using 1.0 g of activated catalyst sample. The

hydrogen flow rate used was 43 ml/min and allowed to stabilize for half an hour. The kinetic data were taken at different temperatures ranging from 523-623 K under different partial pressures of m-xylene. The partial pressure of m-xylene was changed by introducing nitrogen as a diluent. Nitrogen was mixed with the hydrogen/m-xylene mixture and allowed to pass through the catalyst bed. Liquid samples were drawn at interval of 2 hrs and analyzed in GLC for product composition.

### 3.5 Product analysis

Analysis of the liquid samples drawn were performed using a CIC Gas chromatograph fitted with a flame ionization detector. The components of the sample mixture were separated over a 1.6 mm i.d. stainless steel column having a length of 3 m and packed with 5% Bentone - 34, 5% Di-isodecyl phthalate on 60-80 mesh chromosorb W. Pure nitrogen was used as carrier gas. Carrier gas flow rate of 15 ml/min, hydrogen (fuel) gas flow rate of 15 ml/min and a column temperature of 383 K were found to be the best operating conditions for optimum separation of products. A typical chromatogram showing peaks of toluene, p-xylene, m-xylene, o-xylene and trimethylbenzenes is shown in Fig. 4 as a function of retention time. Mixtures containing known amounts of the above compounds were analyzed under the same column conditions. The areas under the peak of the components were found to be directly proportional to the

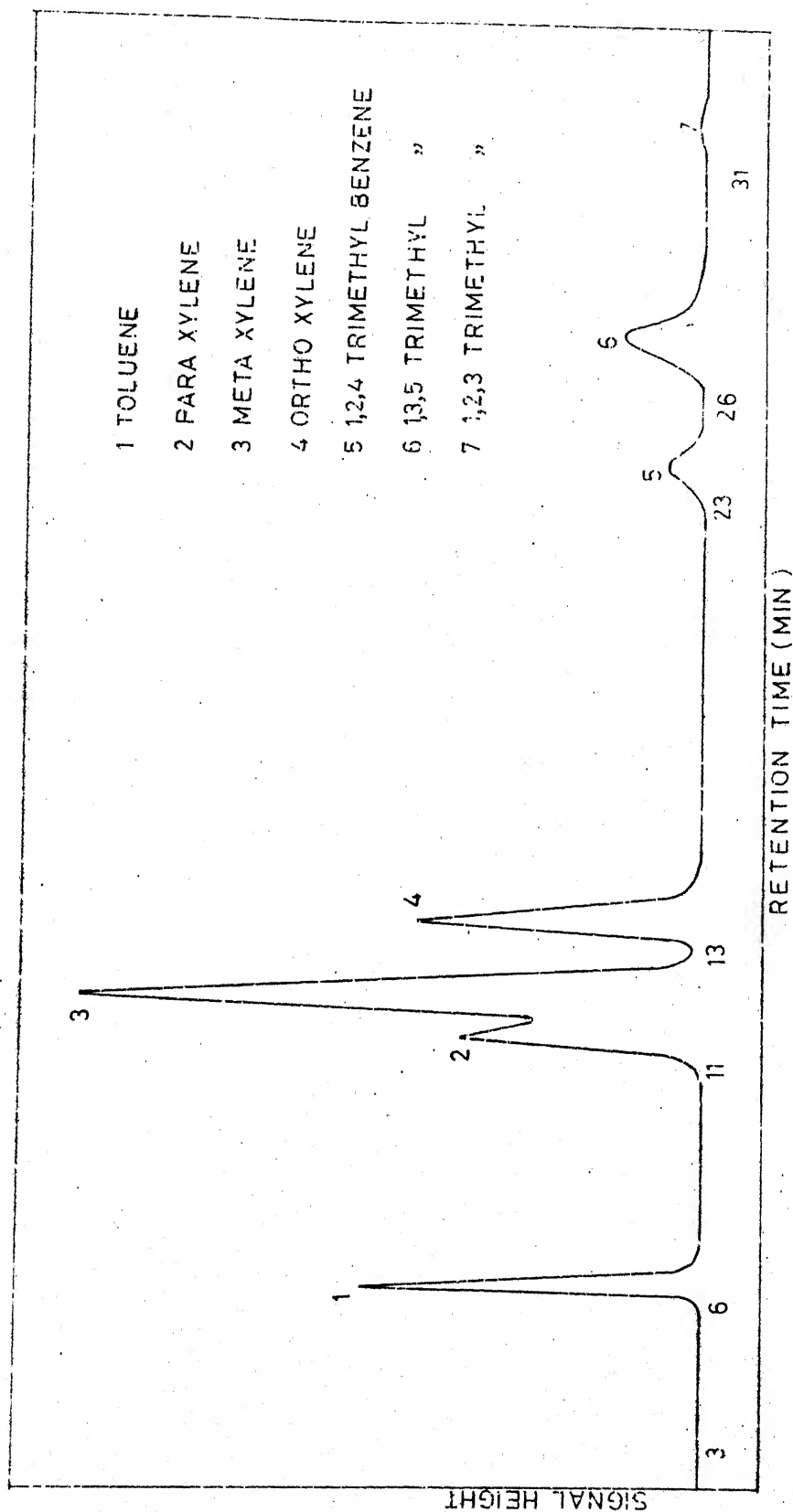


FIG.4 TYPICAL CHROMATOGRAM SHOWING PRODUCT DISTRIBUTION FOR META XYLENE ISOMERIZATION OVER 15% NI-HM CATALYST AT 598 K

respective mole % of the components. Therefore the composition of any component was equated to the ratio of the area under the peak of that component to the sum of the areas of all the peaks appeared.

### 3.6 X-Ray diffraction studies

The X-ray diffraction pattern of various nickel catalysts and the untreated support material was obtained on a horizontal type Siefert diffractometer, employing  $\text{CuK}_\alpha$  radiation. This was done in order to check the loss of crystallinity of the catalysts during pretreatments and reaction conditions. The average nickel crystallite size was also determined for catalysts of various nickel concentrations by the X-ray line broadening technique (37). The X-ray diffraction data for the catalyst samples and the zeolite support were recorded over the range of  $20^\circ$ – $50^\circ$  at a goniometer speed of  $1.2^\circ/\text{min}$  in  $2\theta$  ( $\theta$  = Bragg's angle), a chart speed of  $15 \text{ mm/min}$  and counts per second of  $1\text{K}$ . The nickel (111) peak appeared at  $44.52^\circ$  in  $2\theta$ .

The average nickel crystallite size was determined using the relation given by Klugh and Alexander (37):

$$d_v = \frac{K\lambda}{P_{1/2} \cos \theta} \quad (1)$$

where,  $d_v$  = average crystallite diameter, nm

$K_0$  = crystallite shape factor = 0.9

$\lambda$  = wave length of  $\text{CuK}_\alpha$  radiation = 0.154178 nm

$\beta_{1/2}$  = width of nickel peak at half maximum  
intensity, radians

$\theta$  = Bragg's angle at which the Ni(111) peak appeared  
=  $22.26^\circ$  with  $\text{CuK}_\alpha$  radiation

The specific metal surface area was also calculated from XRD measurements with the assumption of spherical metal crystallites using the relation given below :

$$s = \frac{6}{\rho d_v} \times 10^3 \text{ m}^2/\text{g} \quad (2)$$

where,  $\rho$  = bulk density of nickel metal = 8.90 g/ml

$d_v$  = average crystallite diameter, nm

$s$  = specific metal surface area,  $\text{m}^2/\text{g}$

## CHAPTER 4

### RESULTS AND DISCUSSION

Experimental runs were performed over a series of nickel hydrogen mordenite (Ni-HM) catalysts in vapour phase using pure m-xylene in a fixed bed flow reactor. The present study was conducted in two parts :

- (a) Activity and selectivity studies
- (b) Reaction kinetics and modelling

Catalytic conversion, activity and selectivity are defined as follows :

$$\begin{aligned} \text{Conversion} &= \frac{\text{moles of m-xylene reacted}}{\text{moles of m-xylene fed in the reactor}} \times 100 \\ \text{(mole \%)} & \end{aligned} \tag{3}$$

$$\begin{aligned} \text{Isomerization} &= \frac{\text{moles of m-xylene isomerized}}{\text{moles of m-xylene fed in the reactor}} \times 100 \\ \text{activity (mole \%)} & \end{aligned} \tag{4}$$

$$\begin{aligned} \text{Isomerization} &= \frac{\text{moles of m-xylene isomerized}}{\text{moles of m-xylene reacted}} \times 100 \\ \text{selectivity} & \\ \text{(mole \%)} & \end{aligned} \tag{5}$$

Since p-xylene is an important product, the following terms are also defined :

$$\begin{array}{l} \text{p-xylene} \\ \text{selectivity} \\ \text{(mole \%)} \end{array} = \frac{\text{moles of p-xylene formed}}{\text{moles of m-xylene isomerized}} \times 100 \quad (6)$$

$$\begin{array}{l} \text{p-xylene yield} \\ \text{(mole 3\%)} \end{array} = \frac{\text{moles of p-xylene formed}}{\text{moles of m-xylene fed initially}} \times 100 \quad (7)$$

Experimental runs were also taken with blank hydrogen mordenite support under similar reaction conditions to check its catalytic activity. The reproducibility of experimental data was checked by repeating the experiments under exactly same reaction conditions. The results were found to be reproducible within an error of  $\pm 5\%$ .

In a kinetic study it is very important that mass transfer effects be absent during the reaction in a fixed bed catalytic reactor. Mass transfer effects, both external and pore diffusion were checked in the present study before activity, selectivity and reaction kinetics were studied.

#### 4.1 Mass Transfer Effects

The important variables which can affect the kinetics of the reaction due to diffusion resistance are :

- (a) Space velocity (LWHSV)
- (b) Catalyst particle size

#### 4.1.1 Effect of space velocity (LWHSV)

Effect of external diffusion on conversion was studied by conducting two runs at varying  $\frac{W}{F} \frac{(\text{g.catalyst})(\text{hr})}{(\text{g.mol})}$  but with constant weight of catalyst. The weight of catalyst in one run was double the weight in another run. The conversion vs.  $(\frac{W}{F})$  data for these runs are plotted in Fig. 5. The data for both the runs fall on a single curve, and hence it can be concluded that external mass transfer effects are not important and can be neglected. The minimum flow rates employed in this investigation were 16 cc of hydrogen per min and 0.0143 g.mol of m-xylene/hr. In all subsequent experimental runs flow rates above this value were employed.

#### 4.1.2 Effect of catalyst particle size

To test pore diffusion limitations, conversion vs  $(\frac{W}{F})$  data were obtained for a finely ground catalyst powder and 1.6 mm pellets. The results presented in Figure 6 shows negligible change in conversion with catalyst particle size, thus indicating that pore diffusion resistance is absent. Another criteria (40) was also applied to check the absence of pore diffusion. The effectiveness factor of finely powdered catalyst was assumed to be unity. Based on this assumption the effectiveness factor of 1.6 mm pellet at any level of conversion was calculated using the relation,

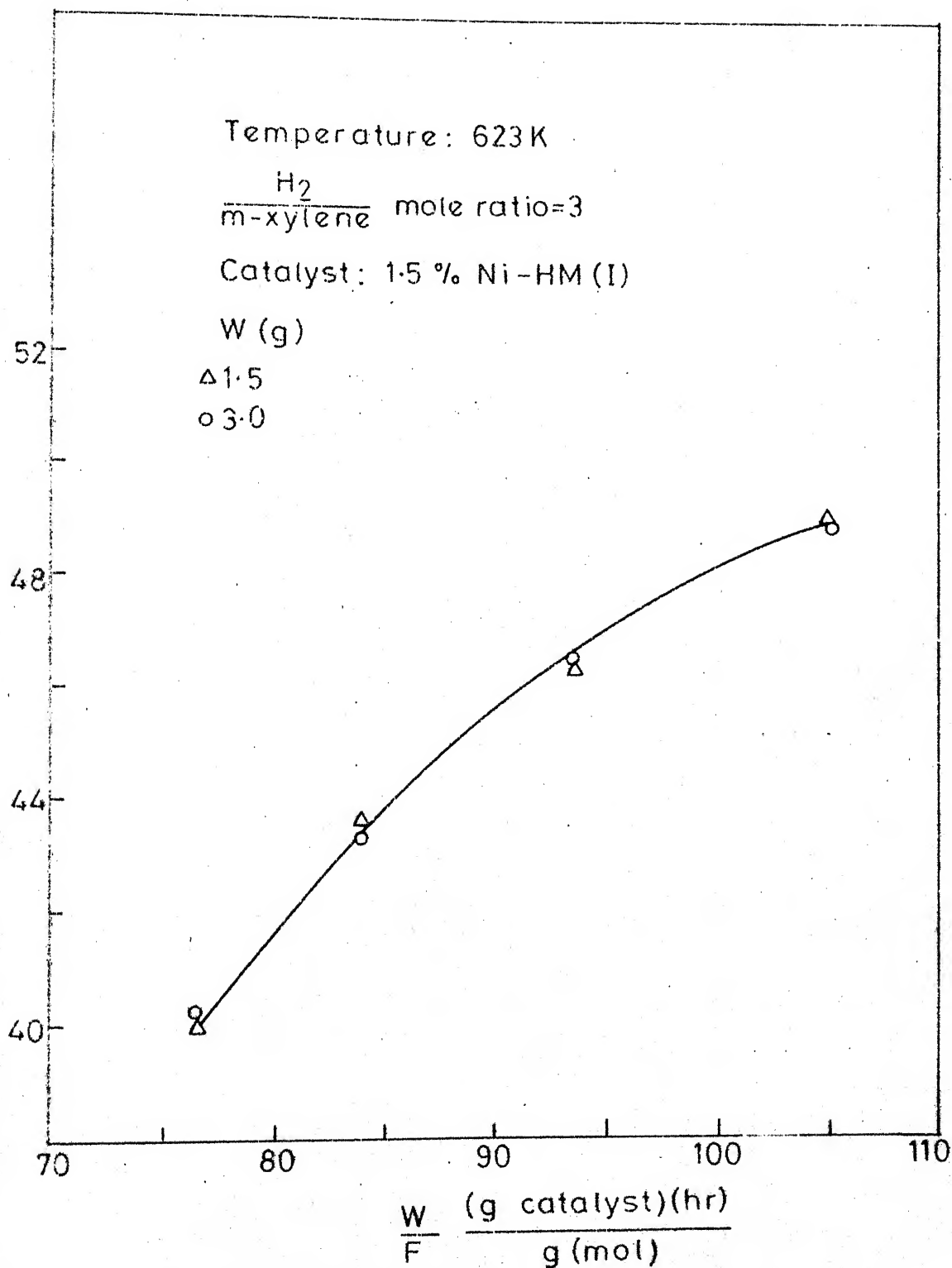


FIG. 5 EFFECT OF (W/F) RATIO ON m-XYLENE CONVERSION

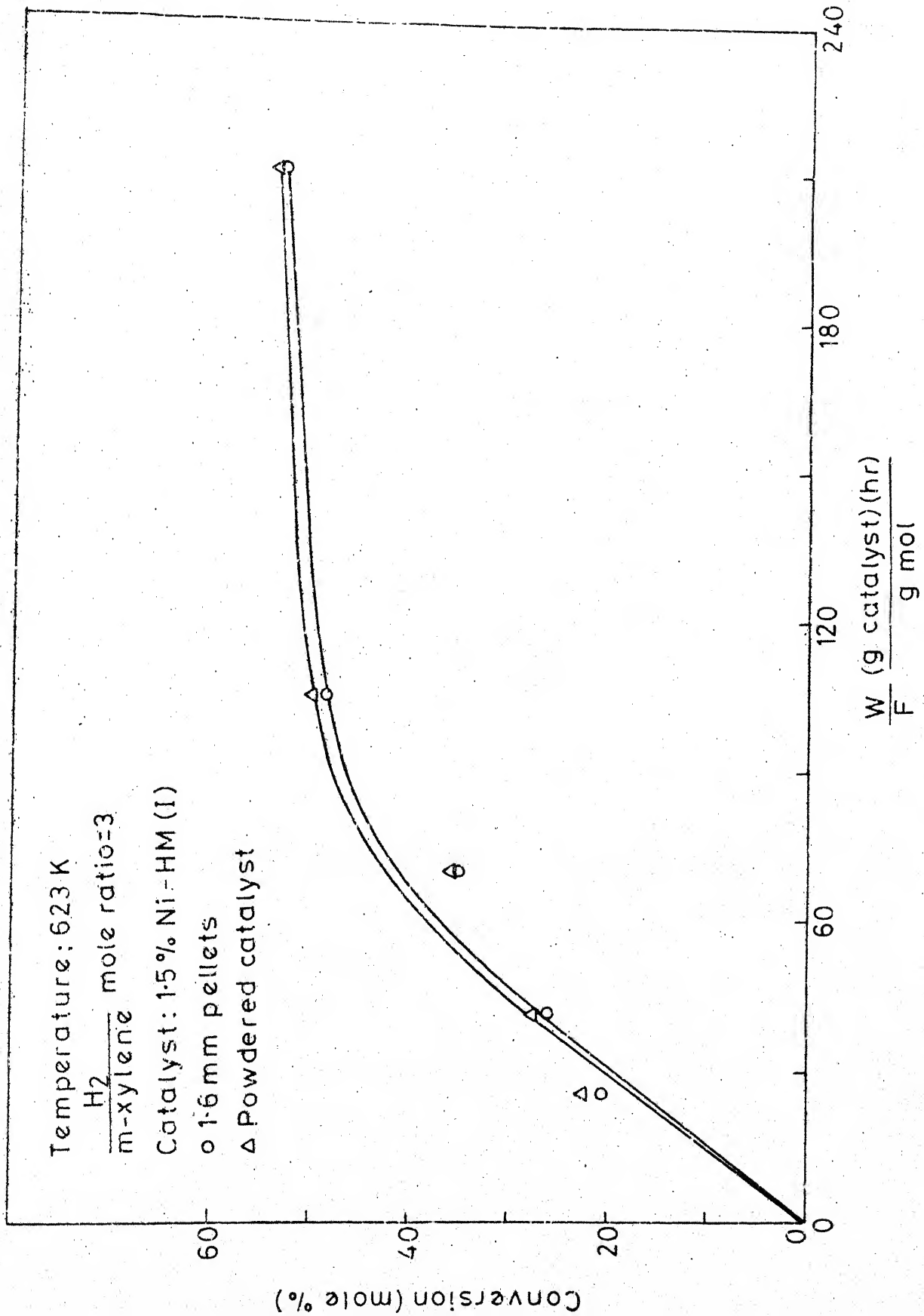


FIG-6 EFFECT OF CATALYST PARTICLE SIZE ON m-XYLENE CONVERSION

$$\eta_1 = \frac{r_1}{r_2} \quad (8)$$

where  $\eta_1$  = effectiveness factor of the given catalyst pellet.

$r_1$  = reaction rate at any conversion level with given catalyst pellet

$r_2$  = reaction rate with powdered catalyst at the same conversion level

For a catalyst of given particle size, the effect of pore diffusion on the reaction rate can be neglected if the value of its effectiveness factor exceeds 0.95 (41).

The reaction rates were calculated from the slope of Figure 6 at different values of m-xylene conversion. These rates are tabulated in Table 1 along with the effectiveness factor values of 1.6 mm catalyst pellet. The average value of effectiveness factor for 1.6 mm pellet was calculated as 0.947 and thus pore diffusional effects can be neglected.

In zeolites which have bimodal pore size distribution, two distinct diffusional processes are involved.

(a) macropore diffusion

(b) micropore diffusion

Micropore diffusional effects cannot be evaluated unless the crystal size of the zeolite is changed. As the diameter of the pores in mordenite is slightly larger than that of the hydrocarbon

TABLE 1 : Comparison of reaction rates of different  
catalyst particle sizes

Catalyst : 1.5% Ni-HM

Reaction : 623 K  
temperature

m-xylene conversion mole%	m-xylene reaction rate g.mol/(hr)(g.catalyst)		Effectiveness factor of 1.6 mm pellet catalyst $\eta_1 = \frac{r_1}{r_2}$
	1.6 mm pellet catalyst $r_1$	Powdered catalyst $r_2$	
0.0	0.85	0.9	0.944
10.0	0.67	0.706	0.949
20.0	0.623	0.651	0.957
30.0	0.595	0.636	0.937

molecules like xylenes, micropore diffusional resistances cannot be ruled out. Since the value of effectiveness factor is close to 0.95, micropore diffusion resistance is probably very small and can be neglected in the present study.

All the subsequent experimental runs were conducted with 1.6 mm catalyst pellets. Since the mass transfer effects were very small, it has not been considered in rate as well as activity studies.

#### 4.2 Activity and selectivity studies

The activity and selectivity of nickel hydrogen mordenite catalysts for m-xylene isomerization were obtained under various operating conditions. Effect of following variables were studied on activity and selectivity of the catalyst.

- (a)  $H_2$ /m-xylene mole ratio
- (b) Liquid weight hourly space velocity (LWHSV)
- (c) Reaction temperature
- (d) Nickel content of the catalyst
- (e) Nickel crystallite size

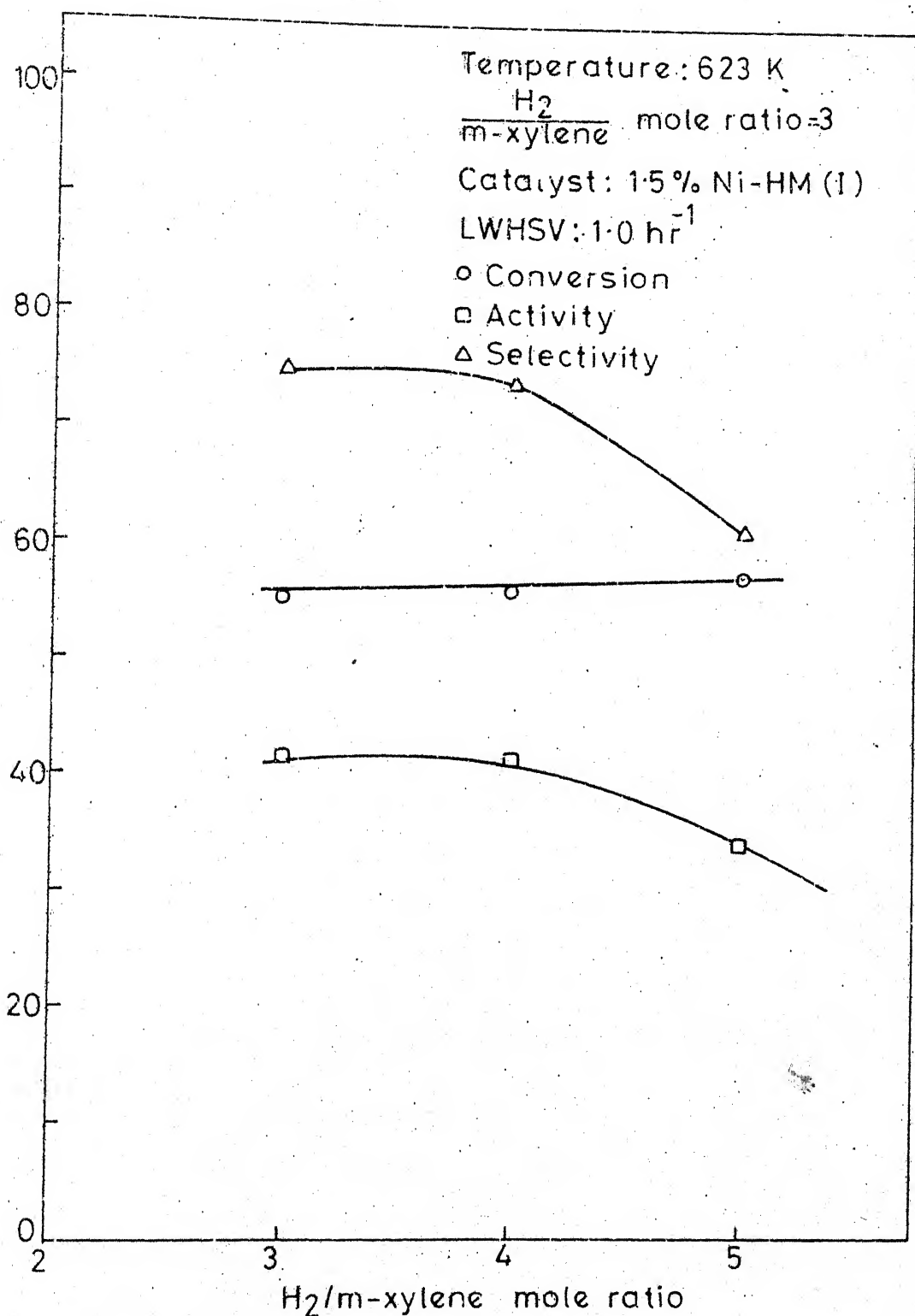
Preliminary experiments performed with various catalysts revealed best activity and selectivity for 1.5% Ni-HM which was in accordance with liquid phase xylene isomerization reported by Sensarma (34). Therefore, 1.5% Ni-HM catalyst was chosen to study the effect of different variables over selectivity and activity.

#### 4.2.1 Effect of $H_2$ /m-xylene mole ratio

The effect of  $H_2$ /m-xylene mole ratio on conversion, isomerization activity and selectivity are plotted in Figure 7. The activity and selectivity decreased with increase in  $H_2$ /m-xylene mole ratio in the range of 3 to 5. The activity dropped from a value of about 42 mole% to 34.5 mole% while the selectivity decreased from a value of about 75 mole% to 61 mole%. The conversion of m-xylene was nearly constant with  $H_2$ /m-xylene mole ratio. The activity and selectivity of the catalyst dropped because of formation of by products at higher  $H_2$ /m-xylene mole ratio due to disproportionation reaction.  $H_2$ /m-xylene mole ratio of 3 was used in all subsequent experimental runs as this showed maximum activity and selectivity for the isomerization reaction. Lower values of  $H_2$ /m-xylene ratio were not used as it may lead to deactivation of the catalyst due to coke formation.

#### 4.2.2 Effect of LHSV

The effect of LHSV on isomerization activity and conversion of m-xylene to para and ortho isomers is shown in Figure 8. An increase in LHSV from 0.5 to 4.0  $hr^{-1}$  results in a decrease in activity and conversion. Higher flow rates of m-xylene at higher LHSV results in a decrease in residence time of the reactants in the catalyst bed, thereby dropping the conversion and activity. Although LHSV value of 0.5  $hr^{-1}$  gave maximum



G.7 EFFECT OF  $\text{H}_2/\text{m-XYLENE}$  MOLE RATIO ON  
CONVERSION, ISOMERIZATION ACTIVITY &  
SELECTIVITY

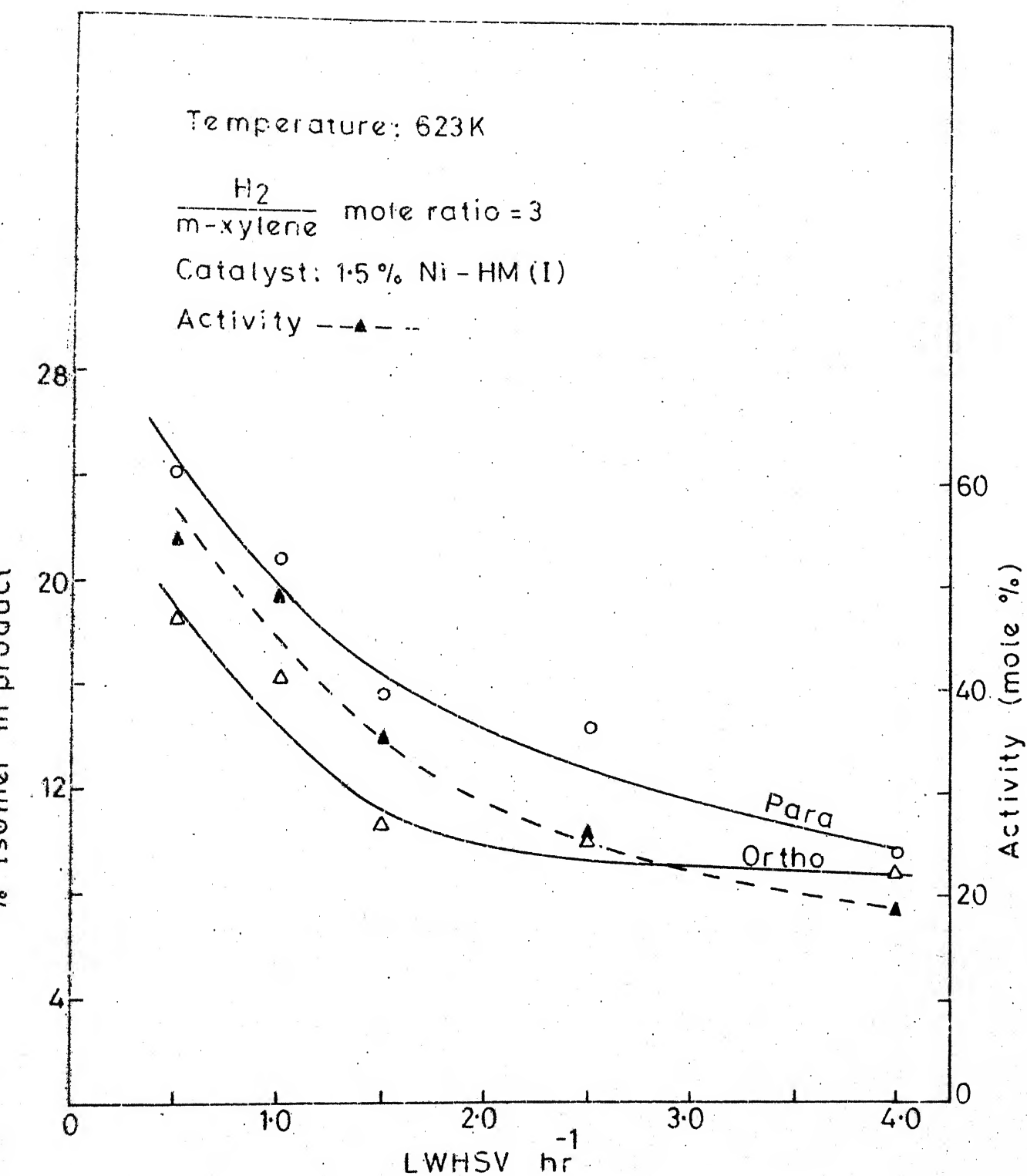


FIG.8 EFFECT OF LWHSV ON ISOMERIZATION ACTIVITY AND CONVERSION OF m-XYLENE TO p-AND-o ISOMERS

conversion and activity, it may probably be in the region of external mass transfer since this corresponds to an  $H_2$  gas flow rate of 16 cc/min and m-xylene feed rate of 0.0143 g.mol/hr. It has already been pointed out in section 4.1.1. that flow rates of  $H_2$  gas and m-xylene above these values ensure absence of external mass transfer. Hence, LWHSV value of  $1 \text{ hr}^{-1}$  (32 cc of  $H_2$ /min and 0.0285 g.mol m-xylene/hr) was used. A value of  $1 \text{ hr}^{-1}$  was used for subsequent studies on activity and selectivity because of appreciable conversion of para and ortho isomers. However, in kinetic studies LWHSV value of  $4 \text{ hr}^{-1}$  was used to get differential conditions of conversion.

#### 4.2.3 Effect of reaction temperature

In order to study the effect of reaction temperature experimental runs were made in the temperature range of 523-623K at constant LWHSV of  $1 \text{ hr}^{-1}$  for 1.5% Ni-HM catalyst. The effect of temperature on conversion, isomerization activity and selectivity of the catalyst are shown in Figure 9. The conversion progressively increased with temperature from 523-623K. The isomerization activity also increased from about 13 mole% at 523K to about 42 mole% at 623K. The isomerization selectivity increased with increase in temperature from 523-573K and decreased with further increase in temperature upto 623K. The selectivity was maximum at 573K and its value was

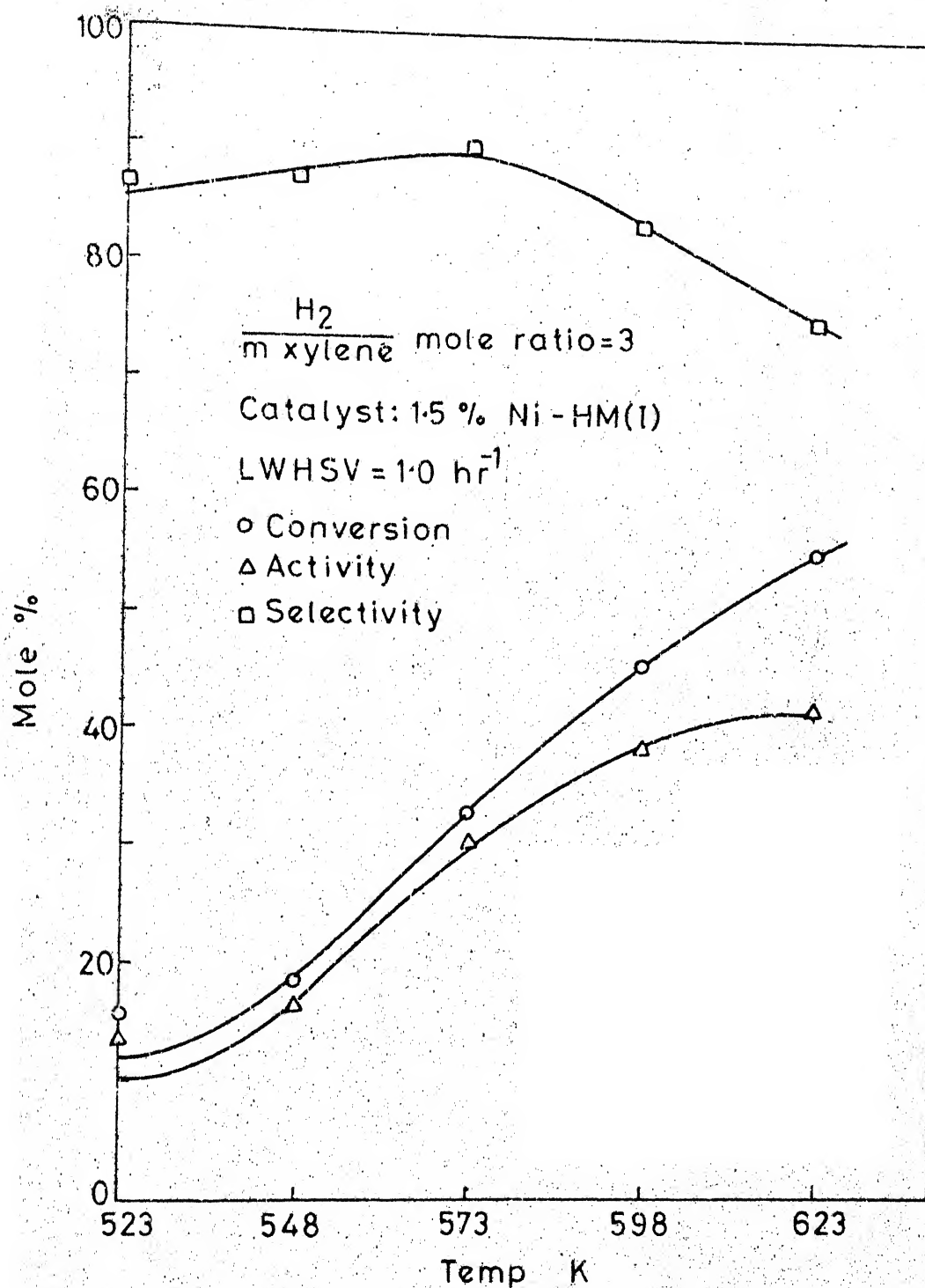


FIG.9 EFFECT OF TEMPERATURE ON CONVERSION, ISOMERIZATION ACTIVITY AND SELECTIVITY

90 mole%.

Plots of the conversion of m-xylene to para and ortho isomers vs. reaction temperature are shown in Figure 10. Figure 10 shows that the rate of p-xylene formation is more than o-xylene formation at a given temperature. The para isomer yield becomes almost constant beyond 598K. Para xylene selectivity was also calculated and found to increase from 50 to 63% in the temperature range of 523-573K. Further increase in temperature dropped the selectivity value to 57.5% at 623K.

The increase in activity and conversion with increase in temperature is due to increase in isomerization rates. The slight increase in selectivity with temperature (523-573K) shows that the disproportionation of xylene is not significant whereas at temperatures above 573K, a drop in the value of selectivity may be due to prominence of disproportionation reaction resulting in the formation of toluene and trimethyl benzene. However, the total yield of disproportionation products were not more than 14 mole%.

Para isomer yield was more than ortho isomer due to para selectivity of the catalyst. The "effective channel apertures" of the mordenite are 8 to 9 Å. The molecular dimensions of the three xylene isomers as found using Fisher-Hirsch-elder-Taylor hard sphere model (41) are 7.0 Å for p-xylene, 7.6 Å for m-xylene and 7.6 Å for o-xylene. Therefore,

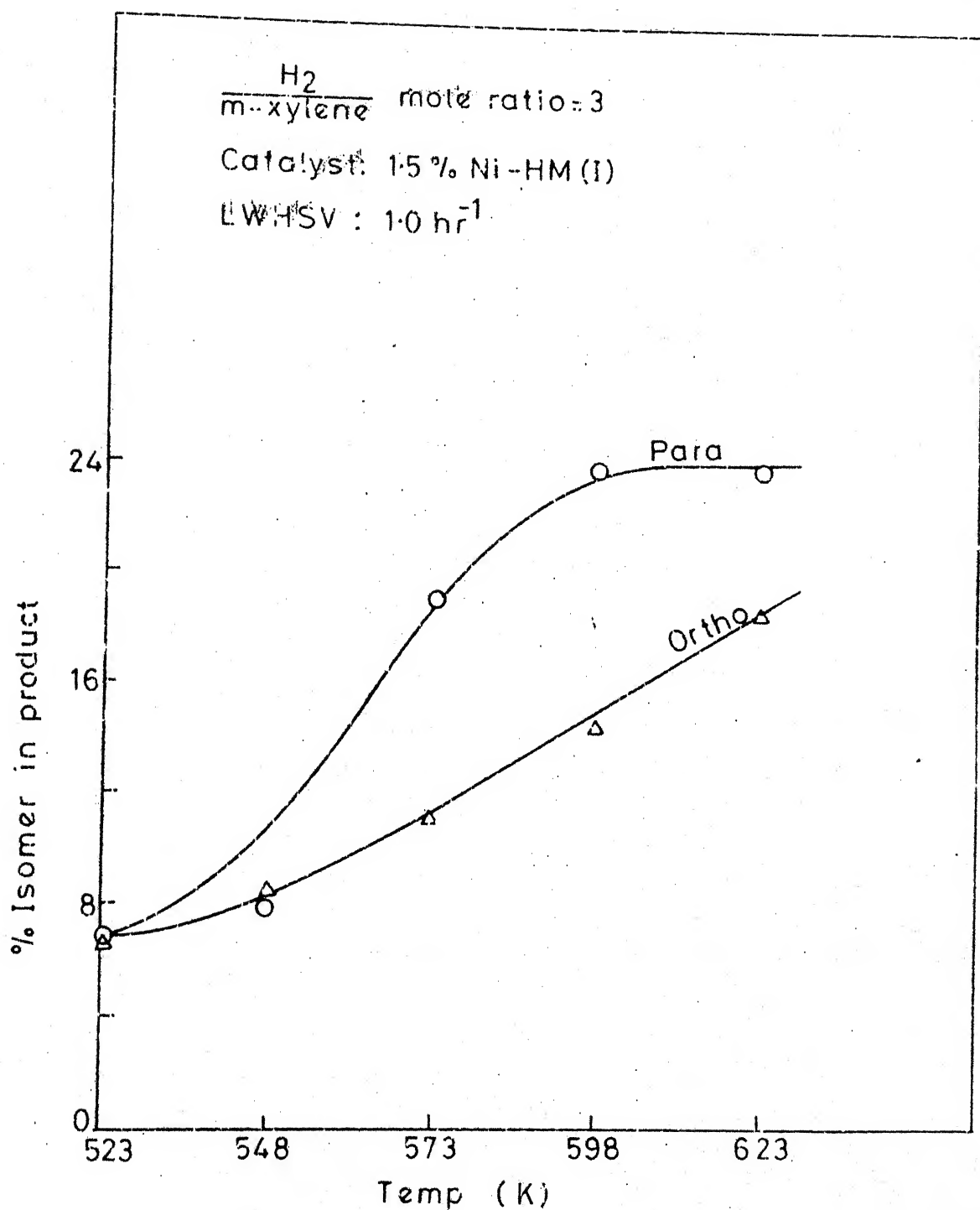


FIG.10 EFFECT OF TEMPERATURE ON CONVERSION  
OF m-XYLENE TO p-AND o-XYLENES

the p-xylene could readily diffuse out of the catalyst pores while the ortho and meta isomers could not do so rapidly. Thus the effective residence time inside the catalyst pore of the more bulky ortho and meta isomers would be increased and would produce more para isomer. A slight decrease in p-xylene selectivity with rise in temperature beyond 573 K may be due to increase of o-xylene diffusivity at a rate faster than p-xylene diffusivity.

Table 2 shows the comparison of activity and p-xylene selectivity with other catalysts reported in literature. The values obtained in the present work were comparable with the reported values. HZSM-5 catalyst gave highest para selectivity because of its pore dimension limitations. Ni-HM catalyst gave higher para selectivity compared to zeolite Y and silica alumina catalysts. Thus Ni-HM seems to be a good choice for isomerization catalyst.

#### 4.2.4 Effect of nickel content

The nickel content was varied from 0.5% to 5% by weight. The conversion, isomerization activity and selectivity of catalysts with different nickel contents were studied at a reaction temperature of 573K and are plotted in Fig. 11. It has already been shown in section 4.2.3 that maximum selectivity was obtained at 573K. The conversion and isomerization activity was found to increase with increase in nickel percentage from 0.5% to 1.5% by weight and reach a maxima. The values decreased with further increase in nickel content upto 3 wt%.

TABLE 2 : Comparison of activity and p-xylene selectivity  
of various catalysts

Catalyst	Activity (mole %) and reaction conditions	p-xylene selectivity $= \frac{\text{para}}{\text{para}+\text{ortho}} \times 100\%$	Reference
Silica alumina	45.4 (755K, Vapour phase)	57.1	16
LaY	23.4 (623K, Vapour phase)	43.0	28
HZSM-5	7.5 (573K, Vapour phase)	64.1	29
1.5% Ni-HM	41.5 (573K, Vapour phase)	58.4	Present Study

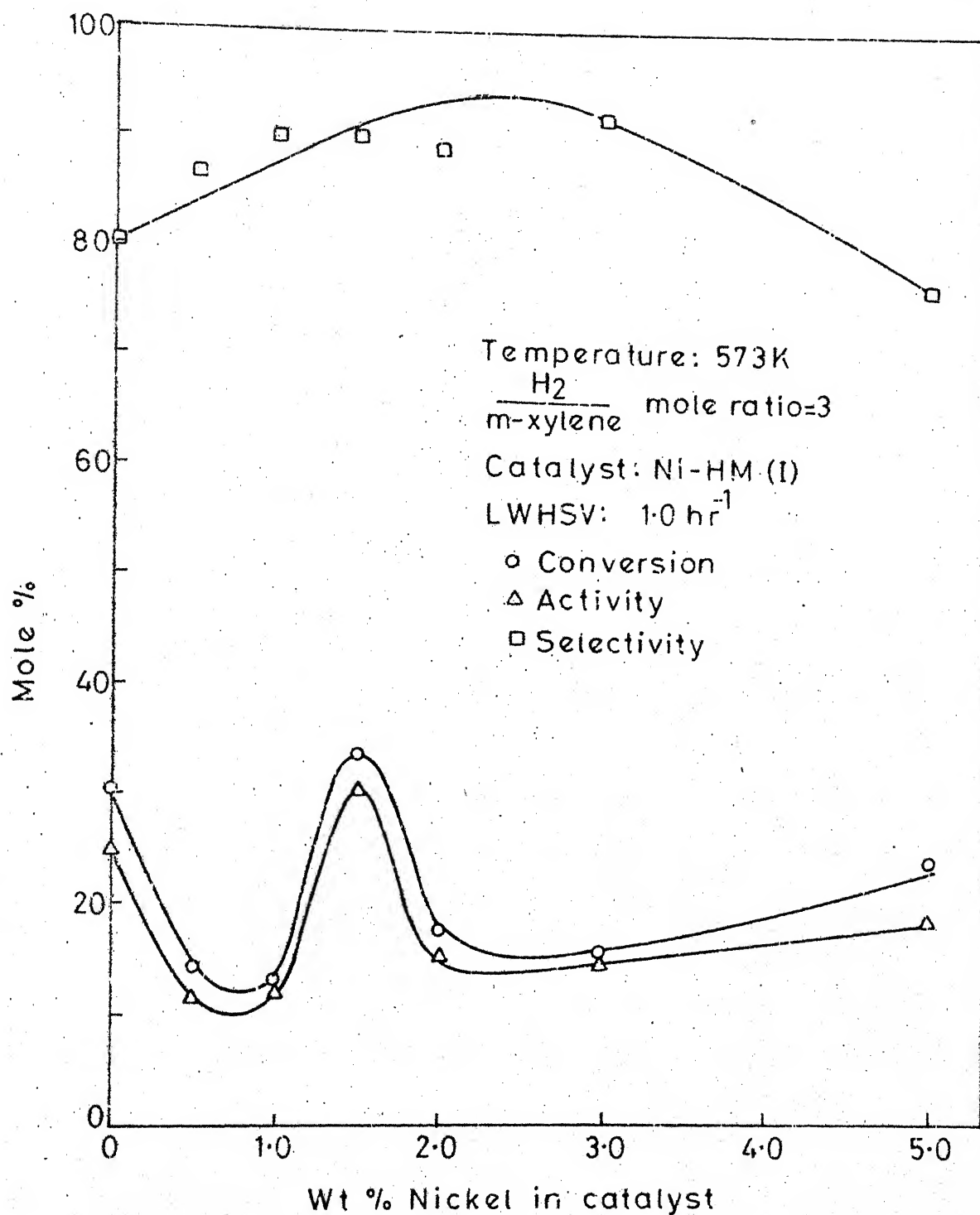


FIG.11 EFFECT OF NICKEL CONTENT ON CONVERSION, ISOMERIZATION ACTIVITY AND SELECTIVITY

5% Ni-HM showed better conversion and activity when compared to 3% Ni-HM. Blank mordenite (0% nickel) also showed appreciable conversion and activity. The isomerization selectivity was found to increase with increase in nickel percentage from 0 to 3% and decreased with further increase in nickel content upto 5%. The isomerization selectivity of 1.5% Ni-HM was 90%.

The turnover number (number of molecules of m-xylene reacted per second per nickel metal site) values were calculated based on the metal area calculated from XRD measurements. The number of metal sites were calculated on the basis of projected area of hydrogen molecule ( $0.120 \text{ nm}^2$  per molecule) and assuming linear stoichiometry of hydrogen adsorption. Hydrogen chemisorption studies were not conducted on these samples. Hydrogen chemisorption can detect the presence of small nickel particles present inside the cavities of mordenite. Since the size of the cavity in mordenite is 0.8 to 0.9 nm and catalysts were prepared by impregnation technique, it is very likely that most of the nickel particles are on the outer surface of mordenite. Therefore, X-ray diffraction gives a fairly good picture of nickel particles dispersed on the outer surface. Thus the metal area calculated from XRD data is justified in calculating turnover number. Table 3 shows nickel crystallite size, metal area and turnover number of various Ni-HM catalyst samples.

The drop in activity and conversion beyond 1.5% nickel may probably be due to the poor utilization of nickel particles present on the outer surface of mordenite. Dispersion of

TABLE 3 : Nickel crystallite size, metal surface area and turnover number of Ni-HM catalysts

% Ni in catalyst	Ni crystallite size nm from X-ray	Ni metal <sup>a</sup> surface area m <sup>2</sup> /g	No. of metal sites per g. of catalyst x10 <sup>-20</sup>	Turnover <sup>b</sup> number x10 <sup>3</sup> (sec <sup>-1</sup> )
0.5	23.86	28.85	2.35	0.986
1.0	22.61	29.82	2.49	1.136
1.5	19.52	34.54	2.88	1.861
2.0	21.48	31.39	2.62	1.079
3.0	19.18	35.15	2.93	0.860
5.0	18.68	36.09	3.01	1.282

$$^a \text{ Nickel metal surface area} = \frac{6}{D_v} \times 10^3 \text{ m}^2/\text{g}$$

$D_v$  = Nickel crystallite diameter, nm

= Bulk density of nickel

= 8.90 g/cc

$$^b \text{ Turnover number} = \frac{\text{No. of m-xylene molecules reacted}}{(\text{metal site}) (\text{sec})}$$

nickel can be affected by number of factors such as degree of reduction of nickel in nickel mordenite catalyst as pointed out by Suzuki et al. (42). 5% nickel gave higher activity and conversion compared to 3% probably due to high degree of nickel reduction leading to better dispersion. However, 1.5% Ni-HM gave maximum value of activity and conversion compared to all catalysts. XRD measurements on 1.5% nickel catalyst reveal the possibility of optimum crystallite size responsible for maximum activity. The crystallite size effect on conversion and activity is discussed in detail in section 4.2.5. Blank mordenite showed appreciable activity because of its acid sites present which are primarily responsible for isomerization reaction. The metallic nickel formed on zeolite surface play a decisive role in the isomerization reaction by suppressing side reactions like disproportionation.

#### 4.2.5 Effect of nickel crystallite size

The average crystallite size was calculated from XRD measurements and the values are shown in Table 3. It is reported in the literature that crystallite size may have an important bearing on the catalytic activity (43). The effect of crystallite size on activity is complicated by several factors such as metal properties, range of crystallite size and method of preparation. The average crystallite size of nickel particles have a marked effect on m-xylene conversion and turnover number

as shown in Figure 12. As the nickel particle size increased beyond 19.5 nm the conversion and turnover number values decreased sharply. The average nickel particle size obtained in the present study was in the range of 18 nm to 24 nm. 1.5% Ni-HM catalyst with crystallite size of 19.5 nm gave maximum conversion and turnover number. These nickel particles which lie on the outer zeolite surface are so large that they behave like metal on other supports. Influence of metal crystallite size on activity of benzene hydrogenation was reported by Coughlan et al. (46) using a series of ruthenium zeolite catalysts.

The effect of nickel metal area on turnover number is shown in Figure 13. Turnover number increased with metal area upto  $34.5 \text{ m}^2/\text{g}$  and beyond this value, the turnover number decreased sharply. 1.5% Ni-HM with a nickel metal area of  $34.5 \text{ m}^2/\text{g}$  showed the highest value of turnover number.

In nickel mordenite catalysts, the formation of nickel crystallites is affected by the presence of acidic hydroxyl group as reported by Suzuki et al. (44). The growth of nickel crystallites on zeolite surface thus depends upon the pretreatment procedures, degree of reduction and hydroxyl groups. Vannice (45) has suggested that with nickel an optimum crystallite size might exist, since large unsupported nickel crystallites have low activity. The observed variation in turnover number is in accordance with Davidova et al. (43)

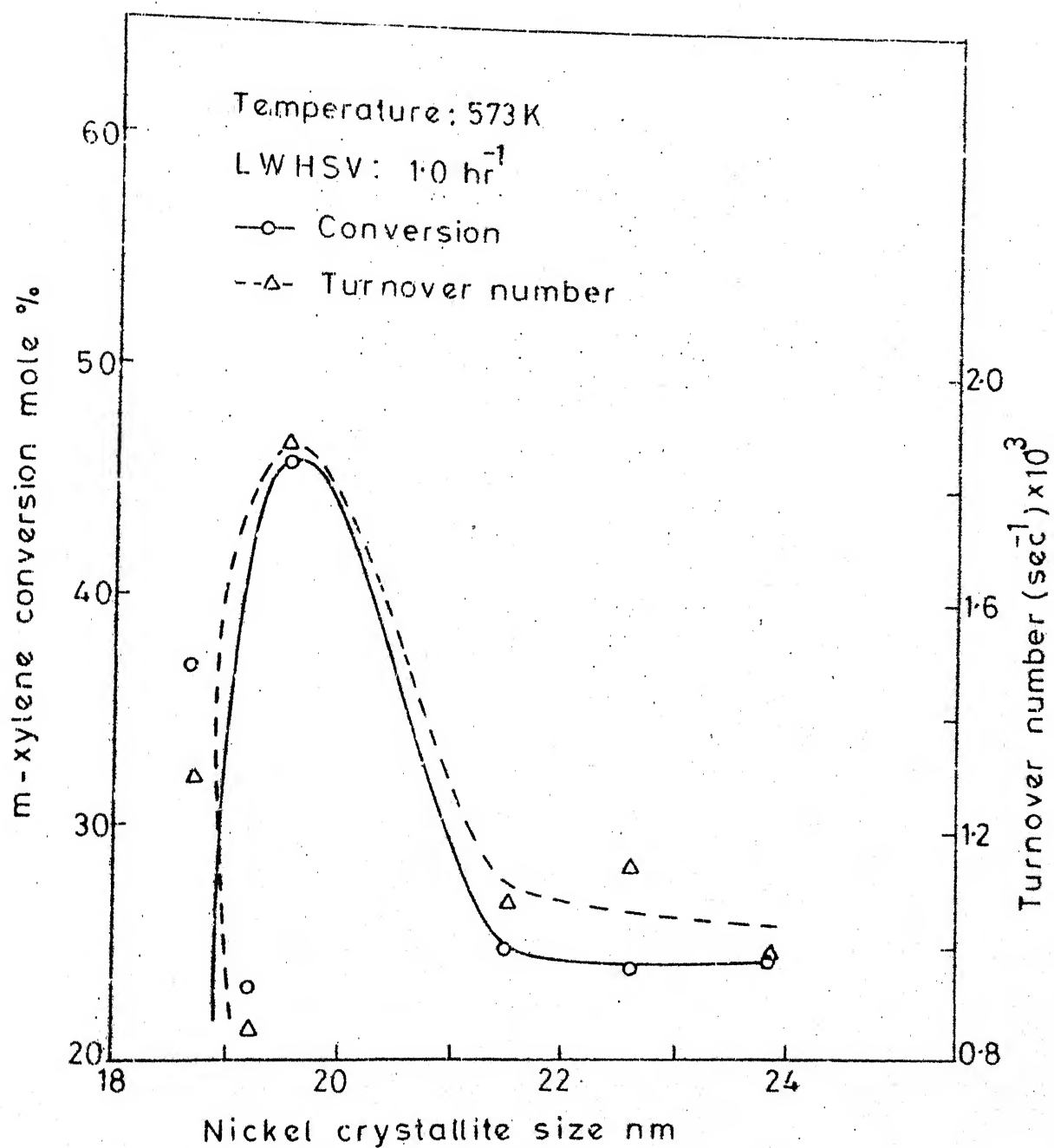


FIG.12 EFFECT OF NICKEL CRYSTALLITE SIZE ON CONVERSION TURNOVER NUMBER

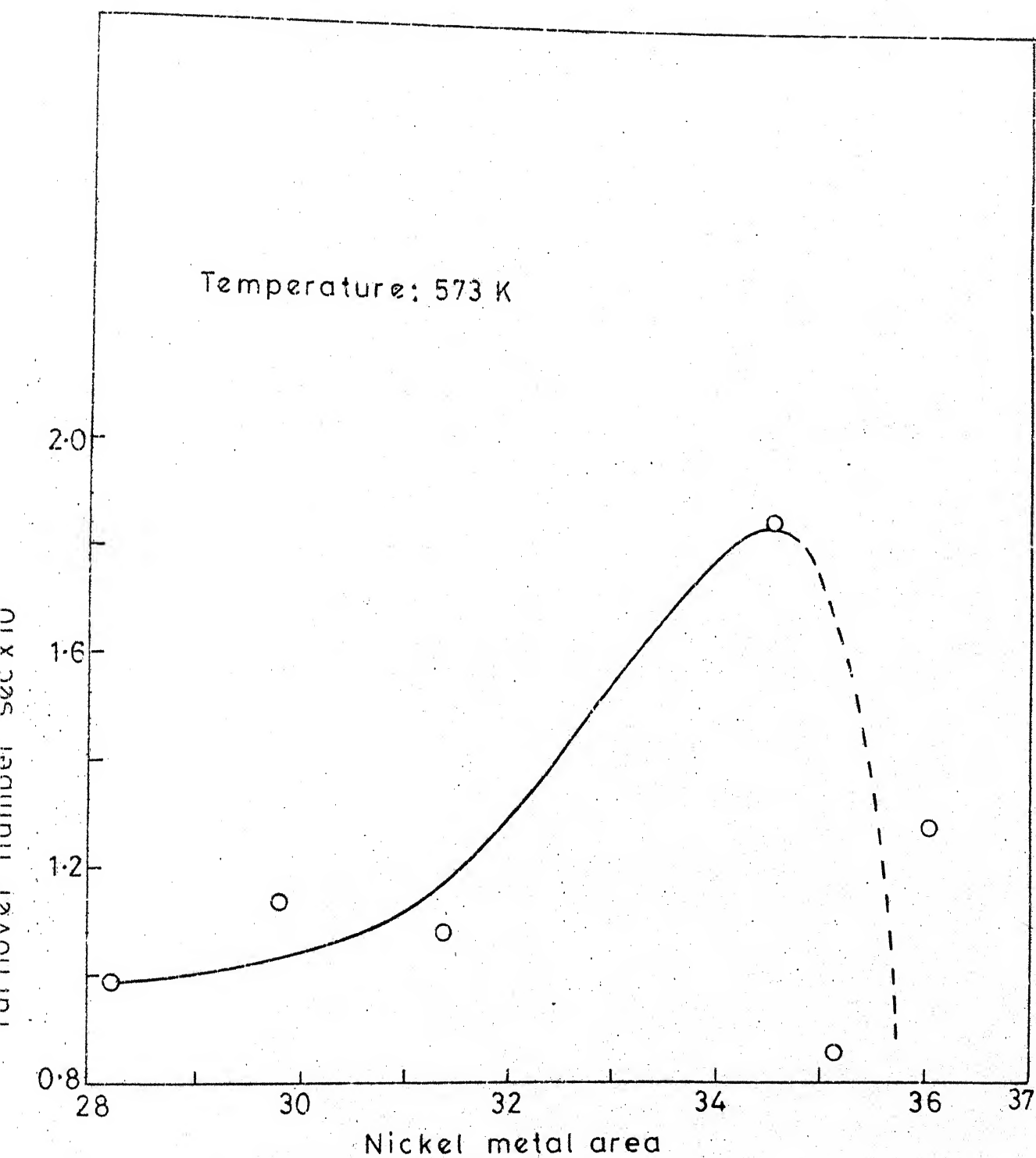


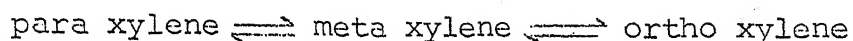
FIG.13 EFFECT OF NICKEL METAL AREA ON TURNOVER NUMBER

who indicated that there exists a definite optimum size of nickel particle in zeolite Y which will give maximum activity for toluene disproportionation.

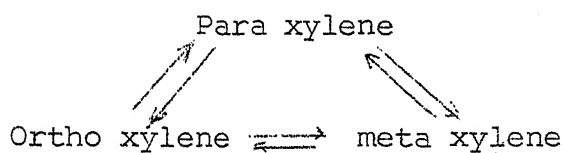
### 4.3 Reaction kinetics and Modelling

Though there are a substantial number of publications concerning the isomerization of xylene over various catalysts, the mechanism of the isomerization reaction is still not very clear. The reaction scheme for the isomerization can be represented as

(i) Series reaction



(ii) Coupled reaction



In the first scheme no interconversion between the para and ortho isomers is considered, where as in the second scheme interconversion among the three isomers is considered.

Both these reactions were successfully applied in number of studies with different catalysts systems in both liquid and vapour phase. For the homogeneous catalyzed reaction using acidic halide catalysts, the investigation led to rather general agreement that isomerization of xylene was series reaction with no interconversion between para and ortho isomers (1-3). Silvestri and Prater (15) calculated the rate constants for the coupled reaction network between the three isomers for the reaction with

silica alumina catalyst. The relative values of these rate constants indicate that the direct conversion of para to ortho and vice versa is very small compared to the conversions of para to meta and ortho to meta isomers. Cortes and Corma (17) also ruled out the possibility of interconversion between ortho and para isomers for the isomerization reaction on silica alumina catalyst. For the same catalyst-reaction system Hanson and Engel (16) also successfully applied the series reaction model. The series reaction model was also applied by Collins et al. (28) and Chutoransky et al. (27) for large pore Y-type zeolite catalysts. With hydrogen mordenite catalyst Hopper and Shigemura (4) calculated the six rate constants according to the coupled reaction scheme for liquid phase isomerization of o-xylene. Their results are consistent with the picture of a system in which isomerization easily takes place in a series of 1,2-methyl group shifts (i.e., meta to ortho and meta to para), but occurs with difficulty in the 1,3-methyl migration (i.e., para to ortho). Miklosy and Papp (6) found their results to be consistent with series reaction scheme for the isomerization of m-xylene using silver exchanged H-mordenite (Ag-HM). Collins et al. (29) found significant interconversion between para and ortho isomers. They concluded that a series reaction mechanism applies to homogeneous silica-alumina and large pore zeolite catalysts but not for the small pore zeolite ZSM-5.

Based on these considerations given above, in the present study of vapour phase isomerization of m-xylene using large pore (0.8-0.9 nm) hydrogen mordenite as catalyst support the series reaction model would be more appropriate for kinetic data analysis. Since in the present work the starting isomer is m-xylene and there is no interconversion between ortho and para isomer, the series reaction can very well be represented as a parallel reaction.

The parallel reaction scheme for m-xylene isomerization can be represented as :



A : m-xylene

R : o-xylene

S : p-xylene

The two xylene isomerization reactions (meta to ortho and meta to para) occur simultaneously and independently, which made it possible to observe the kinetics of both reactions at the same time.

Hougen-Watson formalism, based upon Langmuir Hinshelwood mechanism was used to derive the rate models and are given below for the reaction represented as m-xylene  $\rightleftharpoons$  p-xylene.

Adsorption of A controlling

$$r_S = \frac{k_A \left( P_A - \frac{P_S}{K'} \right)}{(1 + P_S \left( \frac{K_A}{K'} + K_S \right) + K_R P_R)} \quad (10)$$

Single site reaction controlling

$$r_S = \frac{k' \left( P_A - \frac{P_S}{K'} \right)}{(1 + K_A P_A + K_R P_R + K_S P_S)} \quad (11)$$

Dual site reaction controlling

$$r_S = \frac{k' \left( P_A - \frac{P_S}{K'} \right)}{(1 + K_A P_A + K_R P_R + K_S P_S)^2} \quad (12)$$

Desorption of S controlling

$$r_S = \frac{k_S K' \left( P_A - \frac{P_S}{K'} \right)}{(1 + (K_A + K' K_S) P_A + K_S P_S)} \quad (13)$$

where,

$r_S$  = rate of isomerization of m-xylene to p-xylene,  $\frac{\text{g.mol}}{(\text{hr})(\text{g.catalyst})}$

$k'$  = overall rate constant for reaction of m-xylene to p-xylene,  $\frac{\text{g.mol}}{(\text{hr})(\text{g.catalyst})(\text{atm})}$

$k_A, k_S$  = rate constant for adsorption of A or S on  
the catalyst surface  $\frac{\text{g.mol}}{(\text{hr})(\text{g.catalyst})(\text{atm})}$

$K_A, K_R, K_S$  = adsorption equilibrium constants for components  
A, R, S respectively,  $(\text{atm})^{-1}$

$K'$  = homogeneous reaction equilibrium constant.

Similar expressions were derived for the reaction m-xylene  $\rightleftharpoons$  o-xylene.

These rate models were simplified by deleting some of the terms because of their negligible contribution. Table 4 summarizes all the models including simplified ones which were tested for their suitability.

Kinetic runs were made at different temperatures ranging from 523-623K under different m-xylene partial pressures. Liquid weight hourly space velocity of  $4.0 \text{ hr}^{-1}$  was used to ensure absence of diffusional resistance and also to obtain differential conditions of conversion. A typical kinetic data at temperature of 623 K are given in Appendix A.

The effect of partial pressure of m-xylene ( $P_A$ ) on conversion and p-xylene selectivity at different reaction temperatures is shown in Figures 14 and 15 respectively. The partial pressures are the average between inlet and outlet values. The conversion increased at all temperatures as

TABLE 4 : Summary of rate models tested

Rate controlling step	Model	Rate equation for the reaction meta to ortho	Rate equation for the reaction meta to para
1. Adsorption of m-xylene	A-1	$r_R = \frac{k_A \left( P_A - \frac{P_R}{K} \right)}{1 + P_R \left( \frac{K_A}{K} + K_R \right) + K_S P_S}$	$r_S = \frac{k_A \left( P_A - \frac{P_S}{K'} \right)}{1 + P_S \left( \frac{K_A}{K'} + K_S \right) + K_R P_R}$
2. Surface reaction on single site	SS-1	$r_R = \frac{k \left( P_A - \frac{P_R}{K} \right)}{(1 + K_A P_A + K_R P_R + K_S P_S)}$	$r_S = \frac{k' \left( P_A - \frac{P_S}{K'} \right)}{(1 + K_A P_A + K_R P_R + K_S P_S)}$
	SS-2	$r_R = \frac{k \left( P_A - \frac{P_R}{K} \right)}{(1 + K_A P_A + K_R P_R)}$	$r_S = \frac{k' \left( P_A - \frac{P_S}{K'} \right)}{(1 + K_A P_A + K_R P_R)}$
	SS-3	$r_R = \frac{k \left( P_A - \frac{P_R}{K} \right)}{(1 + K_A P_A + K_S P_S)}$	$r_S = \frac{k' \left( P_A - \frac{P_S}{K'} \right)}{(1 + K_A P_A + K_S P_S)}$
	SS-4	$r_R = \frac{k \left( P_A - \frac{P_R}{K} \right)}{(1 + K_A P_A)}$	$r_S = \frac{k' \left( P_A - \frac{P_S}{K'} \right)}{(1 + K_A P_A)}$

TABLE 4 : continued

3. Surface reaction on dual site	DS-1	$r_R = \frac{k(P_A - \frac{P_R}{K})}{(1 + K_A P_A + K_R P_R + K_S P_S)^2}$	$r_S = \frac{k'(P_A - \frac{P_S}{K'})}{(1 + K_A P_A + K_R P_R + K_S P_S)^2}$
	DS-2	$r_R = \frac{k(P_A - \frac{P_R}{K})}{(1 + K_A P_A + K_R P_R)^2}$	$r_S = \frac{k'(P_A - \frac{P_S}{K'})}{(1 + K_A P_A + K_R P_R)^2}$
	DS-3	$r_R = \frac{k(P_A - \frac{P_R}{K})}{(1 + K_A P_A + K_S P_S)^2}$	$r_S = \frac{k'(P_A - \frac{P_S}{K'})}{(1 + K_A P_A + K_S P_S)^2}$
	DS-4	$r_R = \frac{k(P_A - \frac{P_R}{K})}{(1 + K_A P_A)^2}$	$r_S = \frac{k'(P_A - \frac{P_S}{K'})}{(1 + K_A P_A)^2}$
4. Desorption of ortho/para xylene	D-1	$r_1 = \frac{k_R K(P_A - \frac{P_R}{K})}{1 + (K_A + K K_R) P_A + K_R P_R}$	$r_S = \frac{k_S K(P_A - \frac{P_R}{K})}{1 + (K_A + K K_S) P_A + K_S P_S}$

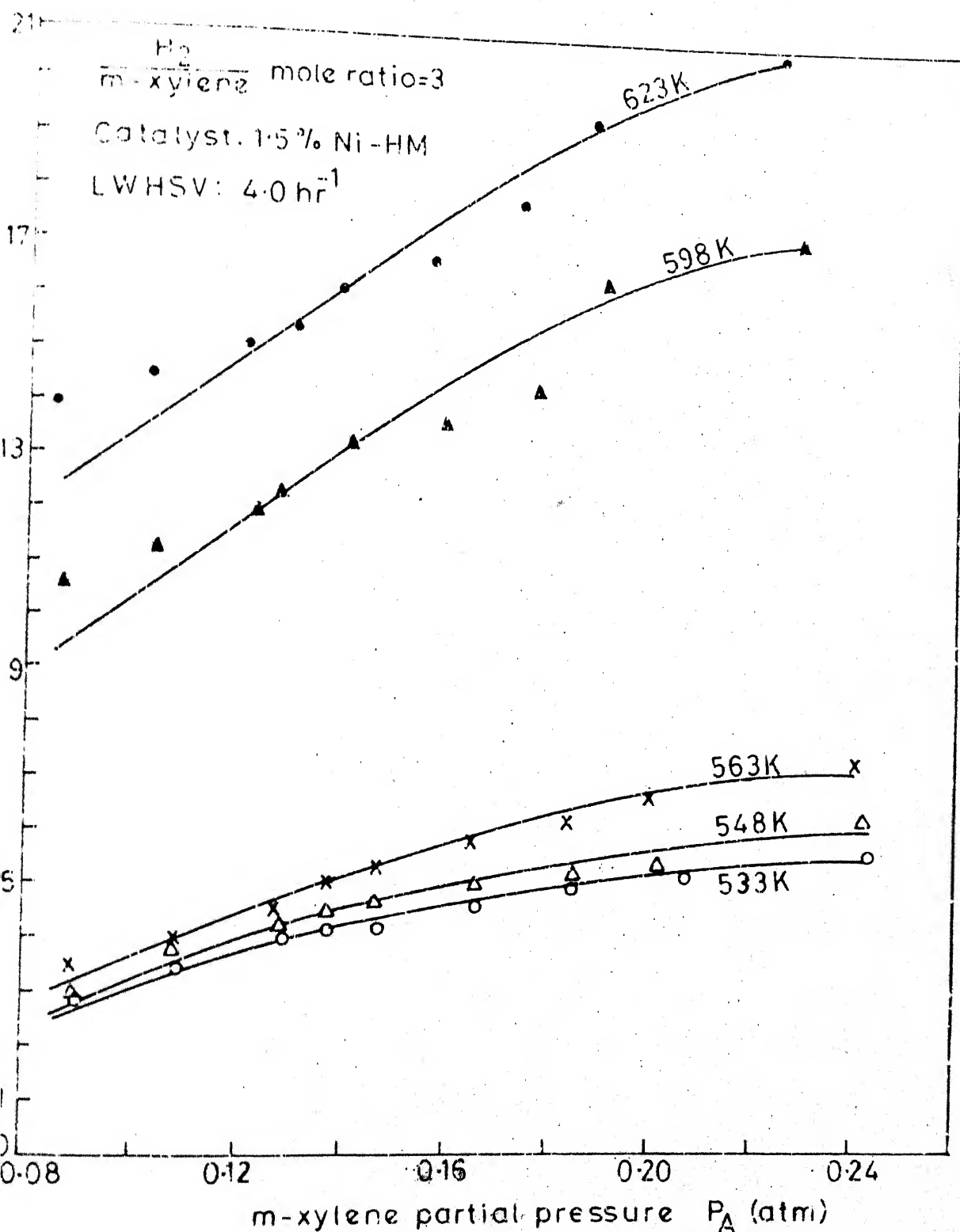


FIG.14. EFFECT OF m-XYLENE PARTIAL PRESSURE ON CONVERSION

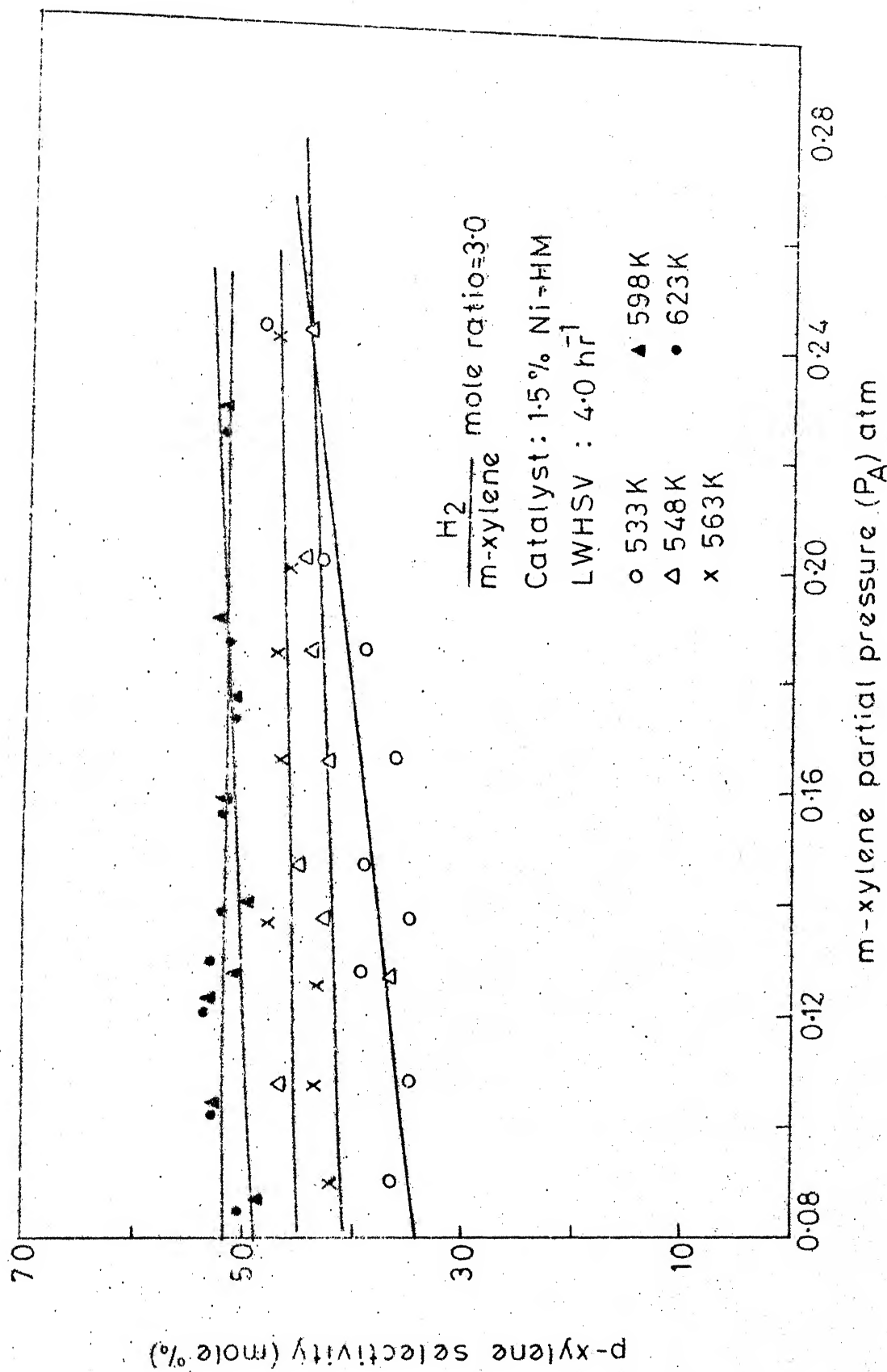


FIG.15 EFFECT OF m-XYLENE PARTIAL PRESSURE ON p-XYLENE SELECTIVITY

the value of  $P_A$  increased whereas the para selectivity remained almost constant. At higher values of  $P_A$ , the concentration of m-xylene in the feed stream is high and hence the conversion is high. As the value of  $P_A$  increases the relative proportions of ortho and para isomers also increased. Since para selectivity is the ratio of para to (Para+ortho) and the reactions (meta to ortho and meta to para) are similar in nature, the para selectivity remained constant.

#### 4.3.1 Mathematical modelling and data analysis

A non-linear regression algorithm utilising Newton-Gauss technique was used to obtain a mathematical fit for various rate models. The program minimized the residual sum of square (R.S.S.) during the regression. The nonlinear computer program basically improved upon the initial estimates of various constants of the rate equation until the R.S.S. could no longer be reduced. The starting values of the parameters were estimated by linear regression. A computer program listing is given in Appendix B.

The model discrimination was done based upon the requirement that kinetic and adsorption constants had to be positive. Some models were rejected on the basis of improper trends of these constants with temperature. The data were most satisfactorily correlated by model DS-4 (surface reaction on dual site rate controlling). Although, this model has close values of RSS compared with SS-4 (surface reaction single site rate

controlling), the choice was based upon the requirement of proper trend of the constants with temperature. Also, the average absolute percentage error for model DS-4 was lower than model SS-4.

Experimental rates were plotted against theoretical rates calculated from model DS-4 for para and ortho isomer formation in Figures 16 and 17 respectively. The experimental rates agreed well with the predicted rates as clear from the Figures. Table 5 gives the values of rate constants and adsorption equilibrium constants of the model DS-4 along with average absolute percentage error and R.S.S. for different temperatures.

The effect of temperature on the rate constants for the isomerization reaction is shown in Figure 18 in the form of Arrhenius plots where the rate constants are plotted against the reciprocal of reaction temperature on a semi log scale. The activation energy of the reaction was calculated from the slope of the straight line. The values of activation energy for para and ortho isomers from meta isomer were found to be nearly same as expected because of the similar nature of the two reactions.

Comparison of activation energy values obtained in the present study with the reported values is shown in Table 6. The activation energies obtained in the present study was slightly lower than the reported values probably due to micropore diffusion limitations in mordenite support.

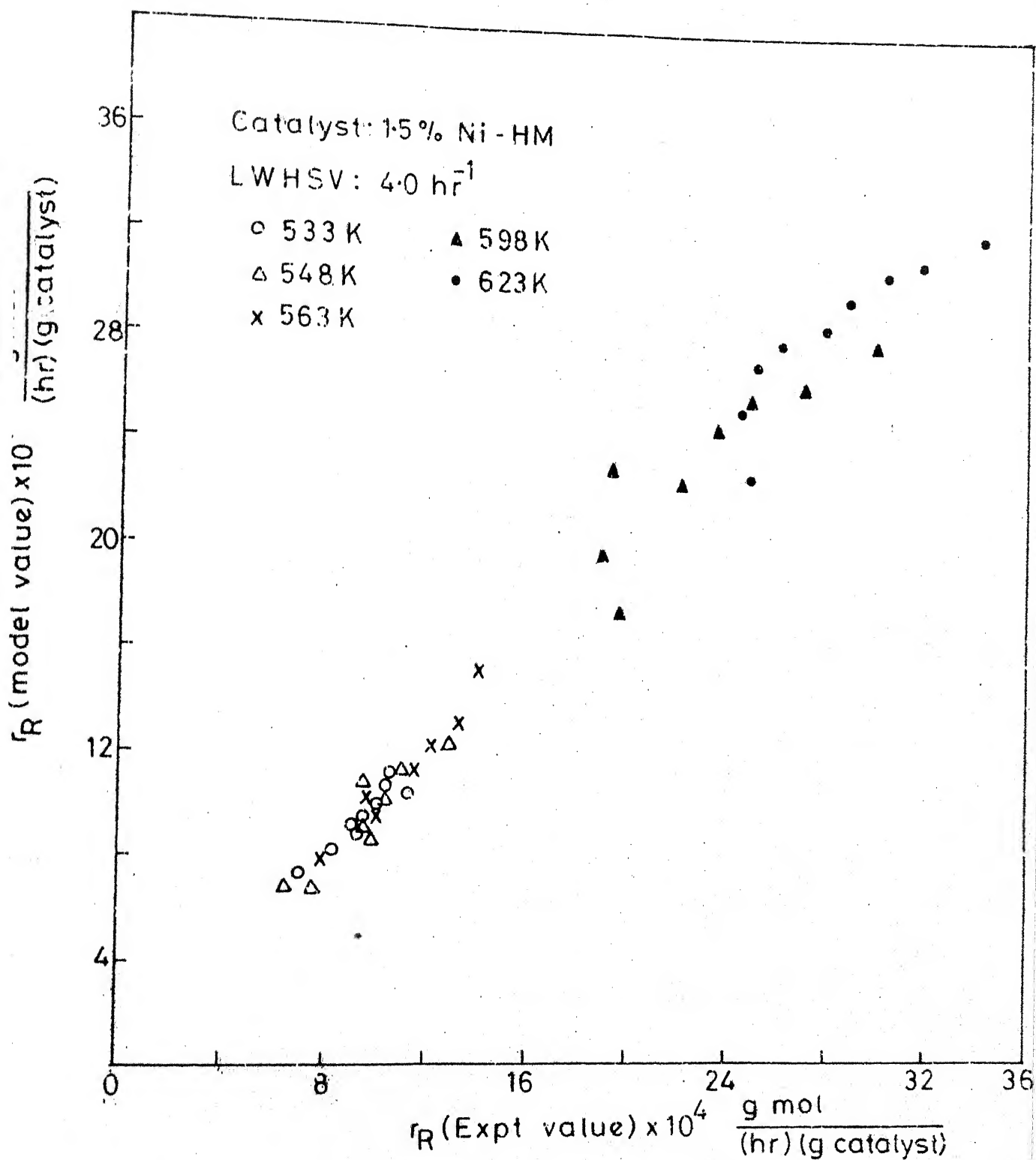


TABLE 5 : RATE CONSTANTS AND ADSORPTION EQUILIBRIUM CONSTANTS OF m-XYLENE ISOMERIZATION  
ON 1.5% Ni-HM CATALYST AT DIFFERENT TEMPERATURES; HYDROGEN TO XYLENE MOLE RATIO 3

MODEL : DS-4

Temperature (K)	Reaction: meta to ortho			R.S.S.	Reaction: meta to para			Aver- age absolu- te % error	R.S.S.
	Rate Cons- tant $k \times 10^2$ $\frac{\text{g.mol}}{(\text{hr})(\text{g.catalyst})}$	Adsorption equilibrium $K_A$ (atm) <sup>-1</sup>	Average absolute % error		Rate Cons- tant $k' \times 10^2$ $\frac{\text{g.mol}}{(\text{hr})(\text{g.catalyst})K_A(\text{atm})^{-1}}$	Adsorption equilibrium constant			
533	1.2677	2.5504	0.1473	$1.3453 \times 10^{-7}$	0.4746	1.432	0.55914	$0.3077 \times 10^{-7}$	
548	0.999	1.5413	0.4082	$0.4632 \times 10^{-7}$	0.7139	1.419	0.73061	$0.3627 \times 10^{-7}$	
598	3.0509	2.1910	0.2113	$0.2536 \times 10^{-6}$	2.9320	1.677	0.098790	$0.77795 \times 10^{-7}$	
623	4.6514	3.1170	0.0944	$0.1815 \times 10^{-6}$	5.229	3.194	0.023085	$0.12418989 \times 10^{-7}$	

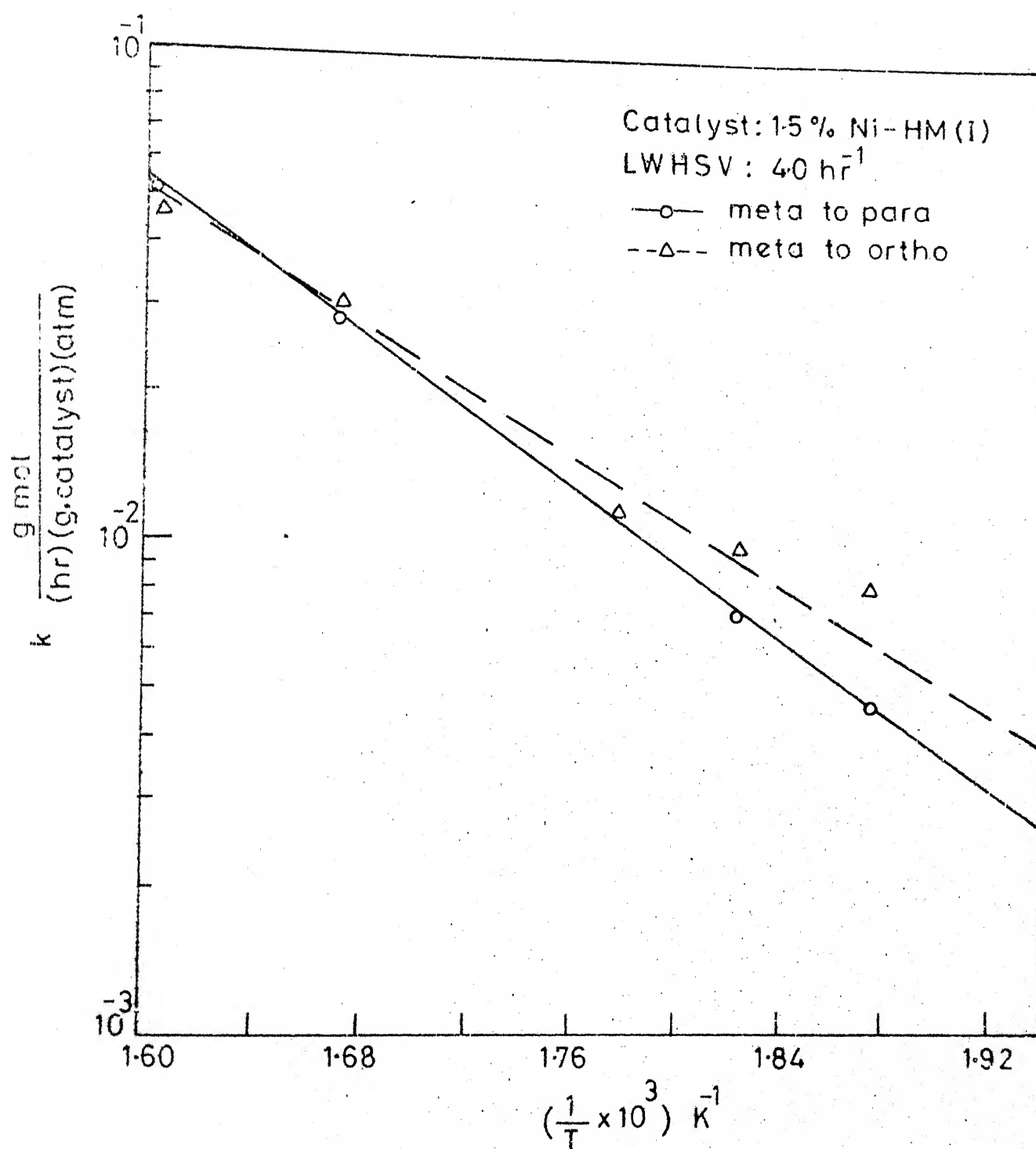


FIG.18 EFFECT OF REACTION TEMPERATURE ON REACTION RATE CONSTANTS (Arrhenius plot)

TABLE 6 : Comparison of activation energies with reported values for the isomerization reaction

Catalyst	Activation energy kcal/mol	Reference
Hydrogen bromide/Aluminium Bromide	22± 1	2
Silica alumina	25.5	16
Hydrogen mordenite	27±2	5
Ag-HM	34-37	6
HI-HM	21-23	34
HI-HM	15-18	Present study

## CHAPTER 5

### CONCLUSIONS AND RECOMMENDATIONS

#### 6.1 Conclusions

Nickel supported on hydrogen mordenite was found to be an active catalyst for vapour phase isomerization of m-xylene.

Conversion of m-xylene remained almost constant with  $H_2$ /m-xylene mole ratio (3 to 5), decreased with increase in LHSV (0.5 to 4  $hr^{-1}$ ) and increased with increase in temperature (523 to 623K). The isomerization activity decreased with  $H_2$ /m-xylene mole ratio, LHSV and increased progressively with temperature. The selectivity decreased with  $H_2$ /m-xylene mole ratio and showed a maxima at a temperature of 573K.

Increase in nickel content of mordenite (0.5 to 1.5%) increased the conversion and activity and showed a maxima around 1.5% nickel. Blank mordenite gave better activity and conversion compared to catalysts having nickel content greater than 1.5%.

A pronounced effect of nickel crystallite size (18-24 nm) was observed on m-xylene conversion. 1.5% Ni-HM catalyst having crystallite size of 19.5 nm gave maximum value of turnover number.

The kinetic data were most satisfactorily correlated by

the model represented as

$$r_S = \frac{k'(P_A - \frac{P_S}{K'})}{(1 + K_A P_A)^2} \quad (\text{meta to para})$$

and

$$r_R = \frac{k(P_A - \frac{P_R}{K})}{(1 + K_A P_A)^2} \quad (\text{meta to ortho})$$

The activation energy for the isomerization reaction was calculated as 15-18 kcal/mol.

It is expected that the present results will contribute to the understanding of kinetics and the role of nickel in Ni-HM catalyst for m-xylene isomerization.

## 6.2 Recommendations

1. Characterization and morphology of nickel particles in Ni-HM catalysts should be studied using other techniques such as Hydrogen gas chemisorption and electron microscopy.
2. A comparative study of Ni-HM catalysts prepared by ion exchange and impregnated techniques should be attempted to study the role of small nickel particles entrapped inside the mordenite cavities.
3. Effect of catalyst preparation variables like calcination temperature, reduction temperature & time should be studied to establish the nickel crystallite size effect on activity and selectivity.

4. Deactivation studies should be carried out with nickel mordenite catalyst to check the decay of activity with time.

REFERENCES

1. McCaulay, D.A., and A.P. Lien, J. Am. Chem. Soc., 74, 6246 (1952).
2. Brown, H., and H. Jungk, J. Am. Chem. Soc., 77, 5579 (1955).
3. Allen, R., and L. Yats, J. Am. Chem. Soc., 81, 5289 (1959).
4. Hopper, J.R., and D.S. Shigemura, AIChE J., 19(5), 1025 (1973).
5. Norman, G.H., D.S. Shigemura, and J.R. Hopper, Ind. Eng. Chem., Prod. Res. Dev., 15(1), 41 (1976).
6. Miklosy, E., J. Papp, and D. Kallo, Zeolites., 3, 139 (1983).
7. Burch, R.G., and A. Voorhies, Ind. Eng. Chem., Prod. Res. Dev., 8, 366 (1969).
8. Dobyanski, A.F., and F.Y. Saprykin, Oil Gas J., 39(13), 48 (1940).
9. Shigeyasu, M., and T. Kitamaura, Jap. Kokai. Pat. 76,115,426 Chem. Abstr., 86: 89351 (1977).
10. Lake, I.J.S., and R.J. Sampson, Ger. Offen, Pat. 2,615,386, Chem. Abstr., 86: 29466 t (1977).
11. Raseev, S., and B. Olteanu, Rev. Chim., 28(6), 521 (1977) Chem. Abstr., 87: 167251 r (1977).
12. Tokaya, H., N. Todo, T. Hosoya, H. Oshio, M. Yoneoka and T. Minegishi, Bull. Chem. Soc. Jap., 45(11), 3662 (1972).
13. Riehm, R.A., U.S. Pat., 4,139,571, Chem. Abstr., 90: 168244 q (1979).
14. Rausch, R.E., U.S. Pat., 4,024,199, Chem. Abstr., 87: 134422 u (1977).
15. Silvestri, A.J., and C.D. Prater, J. Phys. Chem., 68, 3268 (1964).

16. Hanson, K.L., and A.J. Engel, *AIChE J.*, 2, 260 (1967).
17. Cortes, A.; and A. Corma, *J. Catal.*, 51, 338 (1978).
18. Wei, J., and C.D. Prater, *Adv. Catal.* 13, 203 (1962).
19. Hansford, R.C., and J.W. Ward, *J. Catal.*, 13, 316 (1969).
20. Egiazarov, Yu. G., B.N. Isaev, M.F. Savchits, L.L. Potapova, and S.E. Radkevich, *Neftekhimiya*, 17 (6), 842 (1977)  
*Chem. Abstr.*, 88: 88846 f (1978).
21. Bremar, H., F. Hofman, R. Schoedel, and K.P. Wendlandt, *Chem. Tech. (Leipzig)* 27(8), 457 (1957), *Chem. Abstr.*, 83: 16889 n (1975).
22. Sharma, L.D., R.P. Bandoni, P.C. Borthakur, and M.C. Upreti, *Indian J. Chem. Soc.*, 15A (6), 554 (1977).
23. Gajewski, F., and B. Sulikowski, *React. Kinet. Catal. Lett.*, 9(4), 395 (1975).
24. Parasiewicz, K.J., Zesz. Nauk, Univ. Jagiellon, *Pr. Chem.*, 22, 197 (1977), *Chem. Abstr.*, 88: 136216 z (1978).
25. Papp, J., and E. Miklosy, *React. Kinet. Catal. Lett.*, 8(1), 87 (1978).
26. Lanswala, M.A., and A.P. Bolton, *J. Org. Chem.*, 34, 3107 (1969).
27. Chutoransky, P., and F.G. Dwyer, *Adv., Chem. Ser.*, 121, 540 (1973).
28. Collins, D.J., K.J. Mulrooney, R.J. Medina and B.H. Davis, *J. Catal.* 75, 291 (1982).
29. Collins, D.J., R.J. Medina, and B.H. Davis, *Can. J. Chem. Eng.*, 61, 29 (1983).
30. Teijin Petrochemical Industries Ltd., *Jap. Kokai Tokyo Koho Pat.* 80,129,232, *Chem. Abstr.*, 95 : 168757 n (1981).
31. Minachev, K.M., V.I. Garanin, V. Kharlamov, Y.I. Isakova, and E.E. Senderov, *Izv. Acad. Nauk, SSSR, Ser. Khim.* 1737 (1969), *Chem. Abstr.* 72 : 48832 (1970).
32. Beecher, R.G., and A. Voorhies, *Ind. Eng. Chem. Prod. Res. Dev.*, 8, 366 (1969).

33. Inou, T., and M. Sato, J. Jap. Petrol. Inst., 24(5), 160 (1981).
34. Sensarma, P.K., M.Tech. Thesis, I.I.T. Kanpur (1981).
35. Breck, D.W., "Zeolite Molecular sieves", John Wiley & Sons, N.Y., 1973.
36. Satterfield, C.N., "Heterogeneous Catalysis in practice", McGraw Hill Book Company, N.Y., (1981).
37. Klugh, H.P., and L.E. Alexander, "X-ray Diffraction procedures", John Wiley & Sons, N.Y., (1967).
38. Anderson, J.R., "Structure of metallic catalysts", Academic press, London, New York and Sanfransisco (1975).
39. Howie, A., "Characterization of catalysts", Eds., J.M. Thomas, and R.M. Lambert, John Wiley & Sons, (1980), P. 55.
40. Satterfield, C.N., and T.K. Sherwood, "The role of diffusion in Catalysis", Addison Wesley Publishing Company, Inc. (1963).
41. Csicsery, S.M., J. Catal., 23, 121 (1971).
42. Suzuki, M., K. Tsutsumi, and H. Takahashi, Zeolites., 2, 193 (1982).
43. Davidova, N.P., N.V. Peshev, and D.M. Shopov, React. Kinet. Catal. Lett., 16 (1981).
44. Suzuki, M., K. Tsutsumi, and H. Takahashi, Zeolites., 2, 87(1982).
45. Vannice, M.A., J. Catal., 44, 152 (1976).
46. Coughlan, B., S. Narayanan, W. McCann, and W.M. Carroll, J. Catal., 49, 97 (1977).

## APPENDIX A

TABLE A : TYPICAL KINETIC DATA OBTAINED FROM  
EXPERIMENTAL RUN AT 623 K

Catalyst : 1.5% Ni-HM (I)

 $\frac{H_2}{m\text{-xylene}}$  mole ratio = 3 $\frac{W}{F} = 26.16 \frac{(g.\text{catalyst})(hr)}{(g.\text{mol})}$ 

Run No.	Average Partial Pressure <sup>a</sup> (atm)			Reaction: m-xylene to o-xylene		Reaction: m-xylene to p-xylene	
	$P_A$	$P_R \times 10^3$	$P_{H_2}$	$P_{N_2}$	Conversion (XR)	$r_R \cdot \frac{g.\text{mol}}{(hr)(g.\text{catalyst})} \times 10^3$	$r_S \cdot \frac{g.\text{mol}}{(hr)(g.\text{catalyst})} \times 10^3$
1	0.2240	11.1852	0.75	0	7.88	3.4206	3.7315
2	0.1869	8.6394	0.621	0.172	7.12	3.1908	3.4809
3	0.1730	7.5543	0.57	0.24	6.55	3.0397	3.1894
4	0.1558	6.4589	0.51	0.32	6.19	2.9047	3.1687
5	0.1379	5.5078	0.45	0.40	6.21	2.8072	3.0624
6	0.1292	4.8109	0.42	0.44	5.85	2.6272	3.0213
7	0.1202	4.3054	0.39	0.48	5.11	2.5319	2.9317
8	0.1020	3.5627	0.33	0.56	5.00	2.4762	2.78571
9	0.0846	2.9785	0.273	0.636	5.16	2.5023	2.6215

<sup>a</sup> The partial pressures  $P_A$ ,  $P_R$ ,  $P_S$ ,  $P_{H_2}$  &  $P_{N_2}$  are the average between inlet and outlet values.

## APPENDIX B

COMPUTER PROGRAM FOR CALCULATION OF RATE AND  
ADSORPTION EQUILIBRIUM CONSTANTS USING LINEAR  
AND NON-LINEAR REGRESSION ANALYSIS

555

```

DIMENSION PA(20),PR(20),PS(20),RR(20),Y(20)
DIMENSION X(20,20),AP(20)
TPROB=5
DO 200 L=1,NPROB
N=9
PRINT 800,L
READ*,EOC
DO 1 I=1,N
READ*,RR(I),PA(I),PR(I),PS(I)
CONTINUE
TYPE*,EOC
DO 2 I=1,N
TYPE*,RR(I),PA(I),PR(I),PS(I)
N=1
PRINT 801,N
DO 12 I=1,N
K=I
AB(K)=(PA(K)-PS(K)/EOC)
GO TO (5,10,20,26,36,46,56,66,76,86,96,106,116,126),N
Y(K)=1.0/RR(K)
X(K,1)=1.0/AB(K)
X(K,2)=PS(K)/AB(K)
X(K,3)=PR(K)/AB(K)
X(K,4)=RR(K)/AB(K)
X(K,5)=0.0
X(K,6)=0.0
N=4
GO TO 16
Y(K)=1.0/RR(K)
X(K,1)=1.0/AB(K)
X(K,2)=PA(K)/AB(K)
X(K,3)=PR(K)/AB(K)
X(K,4)=PS(K)/AB(K)
X(K,5)=0.0
X(K,6)=0.0
N=4
GO TO 16
Y(K)=1.0/(RR(K)**0.5)
X(K,1)=1.0/(AB(K)**0.5)
X(K,2)=PA(K)/(AB(K)**0.5)

```

```

X(K,3)=PR(K)/(AB(K)**0.5)
X(K,4)=PS(K)/(AB(K)**0.5)
X(K,5)=0.0
X(K,6)=0.0
N=4

```

26

```

GO TO 16
Y(K)=1.0/RR(K)
X(K,1)=1.0/AB(K)
X(K,2)=PA(K)/AB(K)
X(K,3)=PA(K)/AB(K)
X(K,4)=PS(K)/AB(K)
X(K,5)=0.0
X(K,6)=0.0
N=3

```

36

```

GO TO 16
Y(K)=1.0/RR(K)
X(K,1)=1.0/AB(K)
X(K,2)=PS(K)/AB(K)
X(K,3)=PS(K)/AB(K)
X(K,4)=0.0
X(K,5)=0.0
X(K,6)=0.0
N=3

```

46

```

GO TO 16
Y(K)=1.0/RR(K)
X(K,1)=1.0/AB(K)
X(K,2)=PS(K)/AB(K)
X(K,3)=PR(K)/AB(K)
X(K,4)=0.0
X(K,5)=0.0
X(K,6)=0.0
N=3
GO TO 16

```

56

```

Y(K)=1.0/RR(K)
X(K,1)=1.0/AB(K)
X(K,2)=PS(K)/AB(K)
X(K,3)=0.0
X(K,4)=0.0
X(K,5)=0.0
X(K,6)=0.0
N=2

```

66

```

GO TO 16
Y(K)=1.0/RR(K)
X(K,1)=1.0/AB(K)
X(K,2)=PA(K)/AB(K)
X(K,3)=PR(K)/AB(K)
X(K,4)=0.0
X(K,5)=0.0
X(K,6)=0.0
N=3

```

76

```

GO TO 16
Y(K)=1.0/RR(K)
X(K,1)=1.0/AB(K)
X(K,2)=PA(K)/AB(K)
X(K,3)=PS(K)/AB(K)
X(K,4)=0.0
X(K,5)=0.0

```

```

      X(K,6)=0.0
      N=3
      GO TO 16
96    Y(K)=1.0/RR(K)
      X(K,1)=1.0/AB(K)
      X(K,2)=PA(K)/AB(K)
      X(K,3)=0.0
      X(K,4)=0.0
      X(K,5)=0.0
      X(K,6)=0.0
      N=2
      GO TO 16
96    Y(K)=1.0/(RR(K)**0.5)
      X(K,1)=1.0/(AB(K)**0.5)
      X(K,2)=PA(K)/(AB(K)**0.5)
      X(K,3)=PR(K)/(AB(K)**0.5)
      X(K,4)=0.0
      X(K,5)=0.0
      X(K,6)=0.0
      N=3
      GO TO 16
106   Y(K)=1.0/(RR(K)**0.5)
      X(K,1)=1.0/(AB(K)**0.5)
      X(K,2)=PA(K)/(AB(K)**0.5)
      X(K,3)=PS(K)/(AB(K)**0.5)
      X(K,4)=0.0
      X(K,5)=0.0
      X(K,6)=0.0
      N=3
      GO TO 16
116   Y(K)=1.0/(RR(K)**0.5)
      X(K,1)=1.0/(AB(K)**0.5)
      X(K,2)=PA(K)/(AB(K)**0.5)
      X(K,3)=0.0
      X(K,4)=0.0
      X(K,5)=0.0
      X(K,6)=0.0
      N=2
      GO TO 16
126   Y(K)=1.0/RR(K)
      X(K,1)=1.0/AB(K)
      X(K,2)=PA(K)/AB(K)
      X(K,3)=PA(K)/AB(K)
      X(K,4)=0.0
      X(K,5)=0.0
      X(K,6)=0.0
      N=3
      GO TO 16
16    CONTINUE
12    CONTINUE
      CALL SHARMA(Y,X,PA,PR,PS,N,N)
      CALL SHARMA(Y,X,M,N)
      NN=NN+1
      IF(NN.GT.14) GO TO 200
      GO TO 400
200   CONTINUE
      STOP
800   FORMAT(/10X,'PROBLEM NUMBER   = ',I2/)
801   FORMAT(/10X,'MODEL NUMBER    = ',I2/)
      END
C     -----

```

```

C
C SUBROUTINE SHARMA(Y,X,PA,PR,PS,M,N)
C SUBROUTINE SHARMA(Y,X,M,M)
C DIMENSION PA(20),PR(20),PS(20),Y(20),X(20,20),XX(20,20)
C DIMENSION YHAT(20),ERROR(20),SQER(20),XT(20,20),XTX(20,20),
C 1XTY(20),YY(20)
C DIMENSION B(20),BR(20),B1(20,20),AFRE(20)
C 103 FORMAT OF OUTPUT STATEMENTS.
C 104 FORMAT(6(2X,F15.8))
C 19 FORMAT(1X,'THE B VECTOR IS')
C 19 DO 19 I=1,M
C 19 YY(I)=Y(I)
C 18 DO 18 I=1,M
C 18 DO 18 J=1,M
C 18 XX(I,J)=X(I,J)
C 7 CALCULATION OF MEANS
C 5 DETERMINE THE TRANSPOSE OF X
C 5 DO 5 I=1,M
C 5 DO 5 J=1,M
C 6 XT(J,I)=X(I,J)
C 7 FIND XTX(MXM)=XT(NXM)*X(MXM).
C 7 DO 7 I=1,M
C 7 DO 7 J=1,M
C 7 XTX(I,J)=0.0
C 7 DO 7 K=1,M
C 7 XTX(I,J)=XTX(I,J)+XT(I,K)*X(K,J)
C 10 TO FIND INVERSE OF XTX.
C 10 CALL NATINV (XTX,M,B1,0,DETER)
C 11 FIND XTY(N)=XT(NXM)*Y(M)
C 11 DO 11 I=1,M
C 11 XTY(I)=0.0
C 11 DO 11 J=1,M
C 12 XTY(I)=XTY(I)+XT(I,J)*Y(J)
C 12 FIND B(B)=XTX(MXM)*XTY(N)
C 13 DO 13 I=1,M
C 13 B(I)=0.0
C 13 DO 13 J=1,M
C 13 B(I)=B(I)+XTX(I,J)*XTY(J)
C 14 RB(I)=B(I)
C 14 CONTINUE
C 14 PRINT820,(B(I),I=1,M)
C 14 BINTP=YMEAN-B(1)*X1MN-B(2)*X2MN-B(3)*X3MN-
C 14 1B(4)*X4MN-B(5)*X5MN-B(6)*X6MN
C 14 SSR=0.0
C 14 ABER=0.0
C 14 DO 14 I=1,M
C 14 YHAT(I)=B(1)*XX(I,1)+B(2)*XX(I,2)+B(3)*XX(I,3)+
C 14 1B(4)*XX(I,4)+B(5)*XX(I,5)+B(6)*XX(I,6)
C 14 ERROR(I)=Y(I)-YHAT(I)
C 14 ABER=ABER+(ERROR(I)/Y(I))*100.0
C 14 SQER(I)=ERROR(I)**2
C 14 SSR=SSR+SQER(I)
C 15 CONTINUE
C 15 AVABSE=ABER/FLOAT(M)
C 15 PRINT 825,SSR
C 15 PRINT 830,AVABSE
C 825 FORMAT(/10X,'RESIDUAL SUM OF SQUARE = ',E12.5/)
C 830 FORMAT(10X,'AVERAGE ABSOLUTE ERROR = ',E12.5/)
C 820 FORMAT(/10X,'FINAL PARAMETER VALUES '//10X,6(2X,F12.5))

```

```

RETURN
END
SUBROUTINE MATINV (A,N,B,M,DETERM)
ROUTINE FOR MATRIX INVERSION AND SOLUTION OF SIMULTANEOUS EQNS
A-COEFFICIENT MATRIX OF SIZE N
B-CONSTANT VECTOR OF SIZE N
M-NUMBER OF CONSTANT VECTORS
IF M IS SET TO ZERO, ONLY INVERSE IS COMPUTED
DETERM-VALUE OF DETERMINANT RETURNED BY THE ROUTINE
DIMENSION A(20,20),B(20,20),IPIVOT(60),INDEX(60,1)
EQUIVALENCE (IPROW,IRON),(ICOLUMN,ICOLM),(AMAX,T,SWAP)
INITIALIZATION
DETERM=1.0
DO 20 J=1,N
  IPIVOT(J)=0
  SEARCH FOR PIVOT ELEMENT
DO 550 I=1,M
  AMAX=0.0
DO 105 J=1,N
  IF(IPIVOT(J)-1) 60,105,60
DO 100 K=1,N
  IF(IPIVOT(K)-1) 80,100,740
  IF(AMAX-ABS(A(J,K))) 85,100,100
  IRON=J
  ICOLUMN=K
  AMAX=ABS(A(J,K))
CONTINUE
CONTINUE
IPIVOT(ICOLUMN)=IPIVOT(ICOLUMN)+1
INTERCHANGE ROWS TO PUT PIVOT ELEMENT ON DIAGONAL
IF(IRON-ICOLUMN) 140,260,140
DETERM=-DETERM
DO 200 L=1,M
  SWAP=A(IRON,L)
  A(IRON,L)=A(ICOLUMN,L)
  A(ICOLUMN,L)=SWAP
IF(M) 260,260,210
DO 250 L=1,M
  SWAP=B(IRON,L)
  B(IRON,L)=B(ICOLUMN,L)
  B(ICOLUMN,L)=SWAP
INDEX(I,1)=IRON
INDEX(I,2)=ICOLUMN
DIVIDE PIVOT ROW BY PIVOT ELEMENT
PIVOT=A(ICOLUMN,ICOLUMN)
DETERM=DETERM*PIVOT
A(ICOLUMN,ICOLUMN)=1.0
DO 350 L=1,M
  A(ICOLUMN,L)=A(ICOLUMN,L)/PIVOT
IF(M) 380,380,360
DO 370 L=1,M
  B(ICOLUMN,L)=B(ICOLUMN,L)/PIVOT
REDUCE NON-PIVOT ROWS
DO 550 L1=1,M
  IF(L1-ICOLUMN) 400,550,400
  T=A(L1,ICOLUMN)
  A(L1,ICOLUMN)=0.0
DO 450 L=1,M
  A(L1,L)=A(L1,L)-A(ICOLUMN,L)*T
IF(M) 550,550,460
DO 500 L=1,M

```

```

500      B(L1,L)=B(L1,L)-B(JCOLUMN,L)*T
550      CONTINUE
C      INTERCHANGE COLUMNS
600      DO 710 I=1,N
610      L=N+1-I
620      IF(INDEX(L,1)-INDEX(L,2))630,710,630
630      JROW=INDEX(L,1)
640      JCOLUMN=INDEX(L,2)
650      DO 705 K=1,N
660      SWAP=A(K,JROW)
670      A(K,JROW)=A(K,JCOLUMN)
700      A(K,JCOLUMN)=SWAP
705      CONTINUE
710      CONTINUE
      DO 11 K=1,N
      IF(PIVOT(K).NE.1) GO TO 12
      CONTINUE
      RETURN
12      PRINT 991
991      FORMAT(/30X,'MATRIX IS SINGULAR'/)
740      RETURN
      END

```

## ANALYSIS

```

DIMENSION FJAC(20,2),FVEC(20),G(2),S(2),V(2,2),A(43),X(2),T(1)
DIMENSION Y(20),T(20,3)
DIMENSION A(2,2)
EXTERNAL LSQFUN,LSQMON
COMMON Y,T,EQC
C
LW=6*M+4*N+2*M+4*(N-1)/2
DO 500 KK=1,5
  M=2
  READ*,EQC
  READ*,(X(I),I=1,N)
  M=9
  LJ=M
  LV=2
  LIW=1
  LG=43
  TYPE*,EQC
  TYPE*,(X(I),I=1,N)
  DO 20 I=1,M
    READ*,Y(I),(T(I,J),J=1,3)
20  CONTINUE
    DO 3 I=1,M
      TYPE*,Y(I),(T(I,J),J=1,3)
3      IPRINT=1
      MAXCAL=400*M
      ETA=0.5
      XTOL=10.0*SQRT(X02AAF(XTOL))
      STEPMX=10.0
      PRINT 75
      PRINT 85,(X(J),J=1,N)
      IFAIL=1
      CALL E04FCF(M,N,LSQFUN,LSQMON,IPRINT,MAXCAL,ETA,XTOL,STPMX,
        1X,FSUMSQ,FVEC,FJAC,LJ,S,V,LV,NITER,NF,LW,LIS,W,LG,IFAIL)
      PRINT 101,IFAIL
      PRINT 103,(X(J),J=1,N)
      CALL LSQGRD(M,N,FVEC,FJAC,LJ,G)
      DO 121 I=1,N
        DO 121 J=1,N
          A(I,J)=0.0
121      DO 122 K=1,M
          A(I,J)=A(I,J)+FJAC(K,I)*FJAC(K,J)
122      CONTINUE
          PRINT 120
          RSS=0.0
          SSQ=0.0
          DO 40 I=1,M
            DEN=(1.0+X(2)*T(I,1)) ! (M10)
            ANU=X(1)*X(2)*(T(I,1)-T(I,2)/EQC) ! (M10)
            DEN=(1.0+X(2)*T(I,1))*2 ! (M13)
            ANU=X(1)*X(2)*(T(I,1)-T(I,3)/EQC) ! (M13)
            DEN=(1.0+(X(2)/EQC)*T(I,2)) ! (M7)
            ANU=X(1)*(T(I,1)-T(I,2)/EQC) ! (M7)
            SS=ANU/DEN
            FVEC(I)=SS-Y(I)
            SSQ=SSQ+(FVEC(I)/SS)*100
            RSS=RSS+FVEC(I)**2
          PRINT125,SS,Y(I),FVEC(I)

```

```

40 CONTINUE
SSQ=SSQ/M
PRINT 102,RSS
PRINT 110,SSQ
CALL STADEV(X,A,N,M,RSS)
500 CONTINUE
60 STOP
70 FORMAT(10X,'INITIAL GUESS FOR REGRESSION'//)
80 FORMAT(10X,2(2X,E12.5))
101 FORMAT(//10X,'ERROR EXIT TYPE',13//)
102 FORMAT(//10X,'DO EXIT SUM OF SQUARES',E15.8//)
103 FORMAT(//10X,'AT THE POINT',2E15.8//)
104 FORMAT(//10X,'THE ESTIMATED GRADIENT IS',4E15.8//)
105 FORMAT(//10X,'THE RESIDUALS ARE'//)
106 FORMAT(//E15.8)
110 FORMAT(10X,'ABSOLUTE AVERAGE ERROR =',E12.5/)
120 FORMAT(5X,60(1H-)/10X,'MODEL VALUE',5X,'EXPT. VALUE',
15X,'DIFFERENCE'/5X,60(1H-))
125 FORMAT(10X,4(4X,F6.6))
END

```

```

C
C
SUBROUTINE LSQF08C(FLAG,M,N,XC,FVECC,IS,LIN,A,IC)
DIMENSION FVECC(20),W(43),XC(2),IW(1)
DIMENSION Y(20),T(20,3)
COMMON Y,F,ECC
DO 20 I=1,M
DENOM=(1.0+XC(2)*T(I,1)) ! (M10)
ANUM=XC(1)*XC(2)*(T(I,1)-T(I,2)/ECC) ! (M10)
DLI=(1.0+XC(2)*T(I,1))*2 ! (M13)
ANU=XC(1)*XC(2)*(T(I,1)-T(I,3)/ECC) ! (M13)
DEN=(1.0+(XC(2)/ECC)*T(I,2)) ! (M7)
ANU=XC(1)*(T(I,1)-T(I,2)/ECC) ! (M7)
RES=ANUM/DENOM
FVECC(I)=RES-Y(I)
CONTINUE
RETURN
END

```

```

C
C
SUBROUTINE LSQGMN(M,N,XC,FVECC,FJACC,LJC,S,IGRAD,WITER,BF,IA,
ILLW,W,LW)
DIMENSION FJACC(20,2),FVECC(20),S(2),W(43),XC(2),IW(1),G(50)
FSUMSQ=F01DEF(FVECC,FVECC,M)
CALL LSQGRD(M,N,FVECC,FJACC,LJC,G)
GTG=F01DEF(G,G,N)
RETURN
END

```

```

C
C
SUBROUTINE LSQGRD(M,N,FVECC,FJACC,LJC,G)
DIMENSION FJACC(20,2),FVECC(20),G(2)
DO 40 J=1,N
SUM=0.0
DO 20 I=1,M
SUM=SUM+FJACC(I,J)*FVECC(I)
CONTINUE
G(J)=SUM+SUM
40 CONTINUE
RETURN
END

```

```

C -----
C SUBROUTINE STADEV(X,FF,N,M,RSSQ)
C DIMENSION X(2),FF(2,2),FFT(5,5),FY(2)
C INDIC=-1
C DO 10 I=1,M
C DO 10 J=1,N
10 FFT(I,J)=FF(I,J)
C CALL MATINV(N,FFT,FY,INDIC,5)
C SIGMA1=RSSQ/(FLOAT(M-N))
C DO 15 I=1,M
C DO 15 J=1,N
C IF(I.EQ.J) GO TO 20
C GO TO 15
20 FFT(I,J)=SIGMA1*FFT(I,J)
C SD1=FFT(I,J)
C SD1=SQRT(ABS(FFT(I,J)))
C PRINT 302,I,X(I),SD1,RSSQ
302 FORMAT(10X,'X(',I1,')=' ,E15.8,3X,'SD1=' ,E15.8,3X,'RSS=' ,E15.8)
15 CONTINUE
C RETURN
C END
C SUBROUTINE MATINV(N,A,X,INDIC,NRC)
C DIMENSION IROW(5),JCOL(5),JORD(5),Y(5),A(NRC,NRC),Y(N)
C EPS=1.0E-15
C MAX=N
C IF(N.LE.20) GO TO 5
C GO TO 75
5 DETER=1.
C DO 18 K=1,N
C KM1=K-1
C PIVOT=0.0
C DO 11 I=1,N
C DO 11 J=1,N
C IF(K.EQ.1) GO TO 9
C DO 8 JSCAN=1,KM1
C DO 8 JSCAN=1,KM1
C IF(1.EQ.IROW(JSCAN)) GO TO 11
C IF(J.EQ.JCOL(JSCAN)) GO TO 11
8 CONTINUE
9 IF(ABS(A(I,J)).LE.ABS(PIVOT)) GO TO 11
C PIVOT=A(I,J)
C IROW(K)=I
C JCOL(K)=J
11 CONTINUE
C IF(ABS(PIVOT).GT.EPS) GO TO 13
C GO TO 75
13 IROWK=IROW(K)
C JCOLK=JCOL(K)
C DETER=DETER*PIVOT
C DO 14 J=1,MAX
C A(IROWK,J)=A(IROWK,J)/PIVOT
14 CONTINUE
C A(IROWK,JCOLK)=1./PIVOT
C DO 18 J=1,N
C AIJCK=A(I,JCOLK)
C IF(I.EQ.IROWK) GO TO 18
C A(I,JCOLK)=-AIJCK/PIVOT
C DO 17 J=1,MAX
C IF(J.NE.JCOLK) A(I,J)=A(I,J)-AIJCK*A(IROWK,J)
17 CONTINUE

```

```

18 CONTINUE
   DO 20 I=1,N
      IROWI=IROW(1)
      JCOLI=JCOL(1)
      JORD(IROWI)=JCOLI
20 CONTINUE
      IF (INDIC.GE.0) A(JCOLI)=A(IROWI,MAX)
      INTCH=0
      NM1=N-1
      DO 22 I=1,NM1
         IP1=I+1
         DO 22 J=IP1,N
            IF (JORD(J).GE.JORD(I)) GO TO 22
            JTEMP=JORD(J)
            JORD(J)=JORD(I)
            JORD(I)=JTEMP
            INTCH=INTCH+1
22 CONTINUE
         IF (INTCH/2*2.NE.INTCH) DETER=-DETER
         IF (INDIC.LE.0) GO TO 26
         GO TO 75
26 DO 28 J=1,N
      DO 27 I=1,N
         IROWI=IROW(1)
         JCOLI=JCOL(1)
         Y(JCOLI)=A(IROWI,J)
27 CONTINUE
      DO 28 I=1,N
         A(I,J)=Y(I)
28 CONTINUE
      DO 30 I=1,N
      DO 29 J=1,N
         IROWJ=IROW(J)
         JCOLJ=JCOL(J)
         Y(IROWJ)=A(I,JCOLJ)
29 CONTINUE
      DO 30 J=1,N
30 A(I,J)=Y(J)
75 PRINT 301
   DO 45 I=1,N
45 PRINT 302, (A(I,J),J=1,N)
301 FORMAT(/10X,'MATRIX INVERSE IS CALLED'/)
302 FORMAT(10X,3(4X,E15.8)/)
      RETURN
      END

```

**A 83067**

CHE-1984-M-SRE-YAP